

UNIVERSIDAD SAN FRANCISCO DE QUITO USFQ

Colegio de Posgrados

Elevational abundance patterns of bird species in the Ecuadorian Andes: Unraveling the complex drivers

Tesis

María José Arias Saavedra

**Elisa Bonaccorso, PhD
Directora de Trabajo de Titulación**

Trabajo de titulación de posgrado presentado como requisito
para la obtención del título de Magíster en Ecología Tropical y Conservación

Quito, 29 de mayo de 2023

UNIVERSIDAD SAN FRANCISCO DE QUITO USFQ
COLEGIO DE POSGRADOS

HOJA DE APROBACIÓN DE TRABAJO DE TITULACIÓN

Elevational abundance patterns of bird species in the Ecuadorian Andes: Unraveling the complex drivers

María José Arias Saavedra

| | |
|---|--|
| Nombre del Director del Programa: | Elisa Bonaccorso |
| Título académico: | PhD |
| Director del programa de: | Maestría en Ecología Tropical y Conservación |
| | |
| Nombre del Decano del colegio Académico: | Carlos Amilcar Valle Castillo |
| Título académico: | PhD |
| Decano del Colegio: | Colegio de Ciencias Biológicas y Ambientales |
| | |
| Nombre del Decano del Colegio de Posgrados: | Hugo Burgos Yánez |
| Título académico: | PhD |

Quito, 29 de mayo de 2023

© DERECHOS DE AUTOR

Por medio del presente documento certifico que he leído todas las Políticas y Manuales de la Universidad San Francisco de Quito USFQ, incluyendo la Política de Propiedad Intelectual USFQ, y estoy de acuerdo con su contenido, por lo que los derechos de propiedad intelectual del presente trabajo quedan sujetos a lo dispuesto en esas Políticas.

Asimismo, autorizo a la USFQ para que realice la digitalización y publicación de este trabajo en el repositorio virtual, de conformidad a lo dispuesto en la Ley Orgánica de Educación Superior del Ecuador.

Nombre del estudiante: María José Arias Saavedra

Código de estudiante: 00326479

C.I.: 1716402456

Lugar y fecha: Quito, 29 de mayo de 2023

ACLARACIÓN PARA PUBLICACIÓN

Nota: El presente trabajo, en su totalidad o cualquiera de sus partes, no debe ser considerado como una publicación, incluso a pesar de estar disponible sin restricciones a través de un repositorio institucional. Esta declaración se alinea con las prácticas y recomendaciones presentadas por el Committee on Publication Ethics COPE descritas por Barbour et al. (2017) Discussion document on best practice for issues around theses publishing, disponible en <http://bit.ly/COPETHeses>.

UNPUBLISHED DOCUMENT

Note: The following graduation project is available through Universidad San Francisco de Quito USFQ institutional repository. Nonetheless, this project – in whole or in part – should not be considered a publication. This statement follows the recommendations presented by the Committee on Publication Ethics COPE described by Barbour et al. (2017) Discussion document on best practice for issues around theses publishing available on <http://bit.ly/COPETHeses>.

DEDICATORIA

A mi familia, por todo su apoyo y cariño, por enseñarme a amar la naturaleza, y por creer siempre en la fuerza de mis sueños.

AGRADECIMIENTOS

A la Universidad San Francisco de Quito, a la Maestría en Ecología Tropical y Conservación, por el excelente programa y por los fondos de investigación que hicieron posible parte de este estudio, al Colegio de Ciencias Biológicas y Ambientales, y al Laboratorio de Biología Evolutiva.

A Elisa Bonaccorso, por su excepcional tutoría durante este proceso y por creer en mí. Gracias por todo el tiempo y esfuerzo dedicado a la Maestría y a mi trabajo de tesis. Es un placer poder aprender y trabajar contigo.

A Abhimanyu Lele y Jacob Drucker, por su apoyo, sus sugerencias, su ayuda con el análisis de datos, y por llevarme a los bosques y a las montañas. Gracias por compartir su conocimiento y su experiencia, y por permitirme ser parte de este proyecto.

A Stella De La Torre, por sus comentarios y por formar parte de mi comité de tesis. A Benjamin Freeman, por su ayuda con el análisis de datos.

A las reservas e instituciones que nos permitieron realizar trabajo de campo en sus propiedades: Reserva Yanacocha de Fundación Jocotoco, Reserva Orquideológica El Pahuma, Bellavista Cloud Forest Reserve, Reserva Intillacta, Un Poco del Chocó, y Reserva Mashpi de Fundación Futuro.

Finalmente, a mis compañeros y amigos de la Maestría. He disfrutado mucho de este proceso junto a ustedes; gracias por su amistad y cariño.

RESUMEN

La “hipótesis del centro abundante” predice que las especies tienden a ser más abundantes en el centro de su distribución y más escasas hacia los bordes, reflejando la distribución de condiciones y recursos óptimos. Usamos datos de muestreo con redes de neblina y puntos de conteo para estudiar la forma y los factores que controlan la abundancia de 25 especies de aves paserinas en un gradiente de 3000 metros en la vertiente noroccidental de los Andes ecuatorianos, en la zona donde convergen los *hotspots* de biodiversidad de los Andes Tropicales y el Chocó. Modelamos la forma de la distribución de la abundancia a lo largo del gradiente de elevación y utilizamos modelos *N-mixture* para hacer preguntas sobre los parámetros bióticos y abióticos que determinan la abundancia. Mostramos que la distribución de la abundancia de aves en la elevación en estos bosques tropicales de montaña varía entre las especies, y que ningún parámetro predice por sí solo los patrones espaciales locales de abundancia a lo largo del gradiente. Nuestros resultados apuntan hacia el complejo y polifacético sistema de factores ecológicos que configuran la distribución de las especies en los Andes, y refuerzan la necesidad de desarrollar estrategias de conservación más eficaces, imprescindibles para preservar los hábitats de montaña frente al cambio climático y la persistente presión antropogénica.

Palabras clave:

Hipótesis del centro abundante, distribución de abundancia, Chocó Andino, modelos HOF, aves montañas, modelos *N-mixture*, Neotrópicos, Andes Tropicales

ABSTRACT

The “abundant-centre hypothesis” predicts that species tend to be most abundant at the center of their distribution, and scarcer towards the edges, reflecting the distribution of optimal conditions and resources. We used data from mist-net and point count surveys to study the shape and the drivers of abundance of 25 passerine bird species along a 3000-m elevational gradient on the northwestern slope of the Ecuadorian Andes, where the Tropical Andes and Chocó biodiversity hotspots converge. We modeled the shape of the abundance distributions of species across the elevational gradient, and used *N*-mixture models to ask questions about the biotic and abiotic parameters that shape abundance. We show that the elevational distribution of bird abundance in these tropical mountain forests varies among species, and that no single parameter predicts local spatial patterns throughout the gradient. Our results point towards the complex and multifaceted system of ecological factors that shape species’ distributions in the Andes, and they reinforce the need to develop more effective conservation strategies that are imperative to preserve mountain habitats in the face of climate change and persistent anthropogenic pressure.

Keywords:

Abundant-centre hypothesis, abundance distribution, Andean Chocó, HOF models, montane birds, *N*-mixture models, Neotropics, Tropical Andes

Table of Contents

| | |
|--|-------------------------------------|
| Resumen..... | 7 |
| Abstract..... | 8 |
| 1. INTRODUCTION | 10 |
| 2. METHODS | 14 |
| 2.1. Study area and data collection | 14 |
| 2.1.1. Mist-net data | 15 |
| 2.1.2. Point count data..... | 16 |
| 2.2. Data analysis | 17 |
| 2.2.1. Shape of the abundance curve..... | Error! Bookmark not defined. |
| 2.2.2. Predictors of the abundance function..... | 19 |
| 3. RESULTS | 23 |
| 3.1. Shape of the abundance curve..... | 24 |
| 3.2. Predictors of the abundance function..... | 25 |
| 4. DISCUSSION | 28 |
| Conclusions..... | 35 |
| Tables..... | 37 |
| Figure legends..... | 44 |
| Figures..... | 45 |
| References..... | 50 |
| Supplementary Information | 57 |

1. INTRODUCTION

A common focus of biogeography and macroecology has been to describe and understand species' distributions and abundance patterns, and to study the ecological and evolutionary drivers of these patterns (Cox, Moore, & Ladle, 2016). Species are distributed within the geographical ranges that best suit the conditions for their ecological needs (Grinnell, 1917), but their abundances are not uniform across their distribution. Numerous macroecological rules have been posited as depictions that hold true in natural systems at large scales (Gaston, Chown, & Evans, 2008). These rules summarize trends across latitudinal, elevational, and environmental gradients, yet some still lack empirical evidence for their causal mechanisms despite their persistence as common generalities (e.g. the species-energy relationship (Evans, Warren, & Gaston, 2005) and Rapoport's rule (Gaston, Blackburn, & Spicer, 1998)). One such rule describes the distribution of abundance, stating that species tend to be most abundant at the center of their geographic distribution and less so at the edges (Brown, 1984), with the underlying assumption that environmental conditions are most optimal at the center and decline towards the limits (Hutchinson, 1957). This hypothesis, commonly known as the “abundant-centre” hypothesis, predicts that species distributions will be described by symmetric bell-shaped curves with abundance peaking at the geographic center of their range (Brown, 1984). Reviews of studies testing the abundant-centre hypothesis show that most research has focused on temperate taxa in the northern hemisphere (Sagarin & Gaines, 2002) and that empirical tests have found mixed support for the abundant-centre pattern (Dallas, Decker, & Hastings, 2017; Osorio-Olvera, Yañez-Arenas, Martínez-Meyer, & Peterson, 2020; Santini, Pironon, Maiorano, & Thuiller, 2018) which could suggest that the generality of the pattern may not apply to all systems.

The difficulties for methodically testing this hypothesis in natural systems arise from several factors. First, abundance data varies by taxa and sampling methodology, so that accurately comparing large data sets across spatial scales is problematic (e.g., transect sampling, trap capture rates, counts), especially when sampling is carried out in only a portion of a species' known distribution. Second, the delimitation of a species range, whether in geographical or environmental space, is not consistent across studies. Finally, the ways in which distances from range edges to centrality are measured vary substantially. Furthermore, other factors that shape the distribution of abundance are often not considered, such as stochasticity, dispersal ability, species traits, competition, anthropogenic effects, and phylogenetic history (Dallas et al., 2020; Santini et al., 2018). To add to these factors, sampling at a given location does not always allow the detection of a given species, which is why sampling across multiple points in time and accounting for detection processes is important to obtain more accurate estimates of abundance (Royle, 2004).

Despite these disputations, the scientific interest in the abundant-centre has prevailed through time, locations, and taxa (Sagarin, Gaines, & Gaylord, 2006). Recently, Martínez-Meyer et al. (2013) and Osorio-Olvera et al. (2020) found support for the abundant-centre hypothesis by calculating the distance to the niche-centroids in various vertebrate taxa including North American birds, uncovering significant negative relationships between abundance and distance from the niche center in environmental space.

In the Neotropics, mountain systems are characterized by a rapid elevational species turnover (Rahbek, 1997; Terborgh, 1971), narrow elevational ranges (Freeman, Strimas-Mackey, & Miller, 2022; Janzen, 1967), and hump-shaped distribution of species richness (Rahbek, 1997) but see (Herzog, Kessler, & Bach, 2005; Kattan & Franco, 2004; Rahbek, 1995). Shifts in

elevation represent steep changes in environmental conditions over small distances, making tropical gradients excellent systems for testing how biotic and abiotic factors drive spatial patterns of biodiversity and abundance (McCain & Grytnes, 2010; Santillán et al., 2020).

In contrast to the assumptions of the abundant-centre hypothesis, which posits that gradients of environmental suitability shape spatial variation of abundance (Fristoe, Vilela, Brown, & Botero, 2023), accounting for other factors that drive ecological patterns of tropical montane species may explain higher abundances at portions of the range other than the geographic or niche center. For example, the interplay and varying intensity between abiotic and biotic factors in different portions of species' ranges (Jankowski, Londoño, Robinson, & Chappell, 2013; Louthan, Doak, & Angert, 2015) that represent a stress gradient may help explain abundance peaks at range edges. In particular, the distance to the lower elevational limit or “warm” edge of a species distribution may be an indicator of skewed abundance distributions that are shaped by the dynamics at the edges of species' ranges, and which have been associated with elevational patterns of bird richness (Diamond, 1973; Santillán et al., 2018).

Similarly, the influence of anthropogenic pressure is known to affect distribution patterns in tropical mountain ecosystems (Bregman, Sekercioglu, & Tobias, 2014; Riegert et al., 2021). The responses of birds to various types of human-induced disturbances are varied; for example, forest-interior birds are more sensitive to disturbance (O’Dea & Whittaker, 2007). They also exhibit threshold responses in occupancy and habitat use related to canopy cover gradients in the Ecuadorian Chocó (Mordecai, Cooper, & Justicia, 2009), as well as guild-specific responses to habitat loss and disturbance (Durães, Carrasco, Smith, & Karubian, 2013). Habitat specialist birds decline in occurrence probability with increasing human population density (Newbold et

al., 2014), and responses to land-use intensity are dependent on ecological traits (Newbold et al., 2013).

A better understanding of abundance patterns can aid in assessing the portion of a species' range most susceptible to anthropogenic pressures, including climate change (Sekercioglu, Schneider, Fay, & Loarie, 2008). Also, it may aid in identifying source-sink population dynamics along elevational gradients, which may, in turn, inform efforts for the long-term maintenance of "source areas" (Baillie, Sutherland, Freeman, Gregory, & Paradis, 2000; Howe, Davis, & Mosca, 1991; Pulliam, 1988). In addition, abundance data may be useful to assess questions about community assemblages, and serves as a baseline for community, population, and ecosystem monitoring across sites and time (Balmer, 2002; Johnston et al., 2015; Jones, 2011). Finally, the potential changes in the absolute and relative abundance of species along the gradient and across sites may be indicators of the effects of climate change on megadiverse tropical mountain habitats, including lowland biotic attrition and upslope shifts in distribution (Freeman, Scholer, Ruiz-Gutierrez, & Fitzpatrick, 2018).

Despite extensive scientific interest in the biodiversity hotspot where the Chocó and Tropical Andes bioregions converge, no study has systematically analyzed avian abundance patterns in the elevational gradient of this convergence zone. Most studies examining the abundance distributions of species across the globe have done so by testing the abundance patterns across a species' geographic range distribution. In contrast, we take an approach that explores the distribution of species' abundances throughout a local tropical elevational gradient, considering the elevational ranges of species rather than their range-wide distribution, as Freeman & Beehler (2018) did.

Here, we use abundance data from mist-net and point-count sampling throughout a broad elevational gradient on the northwestern slope of the Ecuadorian Andes to test hypotheses about the shape of the abundance distribution of understory passerine species, and the factors that may be driving those patterns. We assess the following hypotheses: (a) that abundance is best predicted by an elevational distance, whether that is the distance to the mid-elevation point of a species' elevational range (as in the abundant-centre hypothesis), or the distance to the lower elevational edge limit (as a response to biotic factors). Regarding the factors that predict the abundance function, we hypothesize (b) that abundance is best predicted by the dynamics of interspecific competition; (c) that abundance is best explained by a measure of anthropogenic pressure; and (d) that abundance is shaped by a combination of some or all these factors.

2. METHODS

2.1. Study area and data collection

Our study was conducted along a 3000-m elevational gradient in the northwest of Pichincha province, in the northern Andes of Ecuador (Figure 1), an area where the biodiversity hotspots of the Tropical Andes and Chocó overlap (CEPF, 2001, 2021; Myers, Mittermeier, Mittermeier, da Fonseca, & Kent, 2000). This region is characterized by the humid tropical montane climate of the Western Cordillera of the Andes. At low elevations, in premontane evergreen forest (300–1400 m a.s.l.), mean annual temperature is 21.6°C and annual precipitation varies between 2075–2704 mm. This forest has canopy height between 25–30 m and abundant lowland arboreal plant species. At the mid elevations of the gradient, in lower (1400–2000 m a.s.l) and montane evergreen forest (2000–3100 m a.s.l), mean annual precipitation varies between 1251–2347 mm, and mean annual temperature between 9.8–16.3°C. The lower montane forest is characterized by closed canopy heights between 20–30 m, palm species and dense herbaceous vegetation

including tree ferns, whereas in the montane forest, canopy height ranges between 20–25 m, and vascular epiphytes such as bromeliads and orchids are predominant, along with regimes of horizontal rain. The high elevations, in upper montane evergreen and *Polylepis* forest (3100–3800 m a.s.l), experience typical high Andean climates, with strong variation in daily temperatures, a mean annual temperature of 7.2°C, and annual precipitation of 1377 mm. The canopy height is slightly lower (15–20 m), but the understory is dense, with abundant epiphytes and higher bryophyte richness (Ministerio del Ambiente del Ecuador, 2013; Ríos-Touma et al., 2022; Teunissen van Manen, Jansen, Cuesta, León-Yáñez, & Gosling, 2019). This region of the Andean-Chocó has a history of severe human disturbance driven by the expansion of agriculture, cattle grazing, deforestation, and mining (Sierra, Calva, & Guevara, 2021).

We obtained abundance data from two sampling methods: mist-nets surveys and point counts. For mist-nets, we sampled high-quality forest habitat exclusively within six nature reserves (Table 1). Point counts were carried out on secondary roads and trails at four different locations along the gradient (Table 2). We defined each geographic sampling location as an “area” and each specific point where we deployed nets or carried out point counts as a “site”. At each site, we recorded coordinates and elevation with a GPS. Each dataset was analyzed separately.

2.1.1. Mist-net data

We deployed mist-nets (2.5 m × 12 m) at 32 sites along the elevational gradient (786–3827 m a.s.l.) at six main locations on the northwestern slope of Pichincha during the months of May, June, and July of 2021 and 2022 (Table 1; Figure 1A). Nets were operated between sunrise and early afternoon, for a total of 7487.5 net-hours. At each site, we deployed 10–15 mist-nets for

three consecutive days, although 22% of sites ($n = 7$) were sampled for less than three days and 25% ($n = 8$) for more than three days. Birds were captured in the field and released immediately after they were processed, measured, and banded with colored plastic rings. Birds were identified using the field guide and taxonomy by Freile & Restall (2018) and measured following methodology described in Pyle (1997). Only first-capture (not recapture) data were included in the analysis.

2.1.2. Point count data

Two different observers familiar with Andean birds carried out fixed radius point-count surveys every 50 m in elevation at 47 sites along the elevational gradient (1350–3800 m a.s.l.), following guidelines detailed in Gilroy et al. (2014) and Mills et al. (2022). Surveys were carried out along the secondary roads Ecoruta El Quinde, in the Tandayapa Valley, along the Mindo road, along trails in Yanacocha Biological Reserve, and along the road descending to Pulumahua Geobotanical Reserve (Table 2; Figure 1B).

Observers recorded time, species observed, abundance, and method of detection (visual or aural) and estimated the distance to each individual within a 50-m radius, calibrating distance with the use of a rangefinder. Weather variables such as temperature, relative humidity, fog, wind, and cloud cover were recorded for each survey. No surveys were conducted during heavy precipitation or in foggy conditions. Surveys lasted for 10 minutes each and data was recorded at 1-min intervals. Four replicates were completed at each elevation between 600 and 1200 h during June, July and August of 2022. In a minority of cases (11%, $n = 5$), sites were visited only three or two times, and two visits at two different sites (4%) occurred during the late afternoon (between 1600 and 1720 h). Observers changed the order in which they surveyed each point to

control for time of day, and each survey was recorded to corroborate unfamiliar bird calls after the survey.

2.2. Data analysis

Because of their higher natural abundances (Callaghan, Nakagawa, & Cornwell, 2021), we only analyzed passerine species with an elevational range breadth that was encompassed by the extent of our surveys, and which had been detected in at least eight sites along the gradient. We sampled up to the tree line at the upper elevational edge of our forest gradient at around 3800 m a.s.l., after which the upper montane evergreen forest becomes predominantly páramo (highland grassland) vegetation (Calderón-Loor, Cuesta, Pinto, & Gosling, 2020). We were thus constrained by the lower edge of the elevational gradient we covered, at 786 m a.s.l., for our selection of species with elevational ranges that were entirely within the extent of our sampling. In addition to this constrain, bird species' local elevational ranges often differ from those in the scientific literature and new geographic and elevational range extensions are continuously updated (Bonaccorso et al., 2011; Freile et al., 2013, 2016). To overcome these challenges, we compared the most recent published elevational ranges for Ecuador (Freile et al., 2022) with our own field data, and kept species whose lowest detection elevation and published lower elevational limit differed by an extent that represented less than 10% of their elevational range breadth. Additionally, we inspected species' local ranges in ArcGIS (ESRI, 2020) using eBird datapoints (2022) from the last 10 years and filtered the occurrence locations to points falling within the Esmeraldas River Basin (CLIRSEN, 2012) which encompasses our elevational gradient of interest. We visually assessed the maximum and minimum occurrence locations of each species using global elevation data (Danielson & Gesch, 2010), considering that noticeably extra-limit observations are records of vagrant individuals.

For each dataset (mist-nets and point counts), we separately calculated species' elevational ranges using our own field data. We calculated the mid-point of their elevational range based on the upper and lower sites where they were detected and calculated the elevational difference between each occurrence elevation and the mid-elevation of their range (hereafter called distance to mid-elevation). Likewise, we calculated the difference between each occurrence elevation and the lower edge of their distribution (hereafter called distance to lower limit).

2.2.1. Shape of the abundance curve

We fit a set of five Huisman-Olff-Fresco (HOF) models to the species' data to nonlinearly assess the shape of the abundance distribution (Huisman, Olff, & Fresco, 1993). Each set of models contains five models of increasing complexity, which describe flat, monotonic, plateau, symmetric, and skewed distributions of abundance across species' elevational ranges (Freeman & Beehler, 2018). We used the Bayesian Information Criterion (BIC) to select the best-fitting model for each species and plotted the best and second-best models within $\Delta \text{BIC} < 2$ of the best model against the abundance data to visually assess model fit. We corrected abundance by sampling effort to account for varying net-hours (Table S3) at different elevations and sites with differing number of point-counts; abundance data for mist-nets was corrected to 100 net-hours and point-counts were standardized to 1 visit (10 minutes). We also used the measure of relative abundance suggested by Freeman (2018). This measure is useful given that mist-net captures rates may not be direct translations of the relative abundance of birds sampled (Remsen & Good, 1996). Thus, since our interest is studying the elevational distribution of abundance of each species, rather than comparing among species, we calculated relative abundance as the capture rate of species at any point in the gradient relative to its own

highest capture rate. We calculated relative abundance in the same way for point count data, using each species' highest observation rate. Finally, we calculated the position of the modeled peak of abundance relative to a scaled elevational range between 0 and 1 divided into thirds (0–0.33, 0.33–0.66, 0.66–1) which we used to aid in the assessment of model fit. This analysis was conducted in R (R Core Team, 2021) using the “nlsLM” function in the “minpack.lm” package (Elzhov, Mullen, Spiess, & Bolker, 2023).

2.2.2. Predictors of the abundance function

To understand the parameters that influence the distribution of abundance along the elevational gradient, we fit N -mixture models (Royle, 2004) to the abundance data using the *pcount* function in the “unmarked” R package (Fiske & Chandler, 2011). N -mixture models are a class of models that allow for the processes of both detection and abundance to be modeled as functions of covariates, where detection is always modeled using the binomial distribution and abundance may be modeled under various distributions (Kéry, Royle, & Schmid, 2005). For spatially replicated count data, such as those obtained through mist-net and point count surveys, one can record variables that differ with each independent visit (i.e., visit-level) and those that vary by site (i.e., site-level), and select combinations of those covariates to model the detection and abundance functions, respectively. We took an approach where we first tested visit-level covariates for the detection function of each species' data without abundance covariates, and then selected the best-fitting combination of visit-level (i.e., detection) covariates to model the abundance with site-level covariates.

For mist-net data, we included net-hours as a visit-level covariate in all models, including the null model, to account for differences in sampling effort throughout the netting sites in the

study area. Date, recorded as the number of days since the first day of the year, and day of netting at a given site (i.e., first day, second day, etc.) were also included as visit-level covariates. Date accounts for seasonality and day of netting accounts for differences caused by decreased capture rates due to net-avoidance (MacArthur & MacArthur, 1974; Marques et al., 2013). We tested four visit-level covariate combinations to model the detection process for each species with null site-level covariates and selected the best-fitting combination to subsequently fit abundance models. Visit-level covariates for point-count data models were date, temperature, cloud cover, observer identity, and time of day. For survey data, time of each survey was converted into minutes after sunrise, as bird detections tend to decrease in the hours after the sun rises (Esquivel Mattos & Peris, 2008). We tested 32 detection covariate combinations and used the best supported combination to fit abundance models.

Our most complex model structure included 3 of 5 site-level covariates: one of two elevational distances (distance to mid-elevation or distance to lower elevational limit), Population Gravity Index (PGI) (Hoover & Giarratani, 1971; Polyakov, Majumdar, & Teeter, 2008) as a measure of anthropogenic disturbance in the study area, and presence/absence data for one of two competitors (in terms of phylogenetic or morphological distance). The two elevational distances were not tested in the same model (as they are entirely confounded), and neither were the two potential competitors (in cases where the identity of the closest phylogenetic competitor did not coincide with the morphological competitor).

PGI is intended to capture the additive effects of all populated places around a particular site,

$$\sum PGI_i = \frac{P_k}{D_{ki}^2}$$

where PGI_i is the PGI for site i , P_k is the population of each populated place k within a determined radius of site i , and D_{ki}^2 is the squared distance between site i and populated place k . All the PGI values for site i are then added for the resulting gravity index. However, we found little variability in the $\sum PGI$ values for our field sites, so we used only the closest populated place as a proxy for the effects of anthropogenic pressure on abundance. PGI was thus calculated as follows:

$$PGI_i = \frac{P_k}{D_{ki}^2}$$

Distances to nearest populated places within a 25-km radius of each study site were calculated using the Near analysis tool in ArcGIS Pro 3.0.0 (ESRI, 2020), and then scaled with the base R package (v 4.1.2.). Population data was obtained from INEC (2010), and populated places were defined as census blocks representing parish or canton seats, or concentrations of few houses.

Studies often assume that closely related bird species compete and drive patterns of elevational distributions (Jankowski, Robinson, & Levey, 2010). Nonetheless, species that are more similar morphologically rather than genetically may also impose competition (Stevens & Willig, 2000). Therefore, we considered the closest morphological or phylogenetic competitor to each of our focal species, with the caveat that the phylogenetic competitor may correspond with the identity of the morphological competitor, given that morphology is often phylogenetically conserved (Webb, Ackerly, & McPeck, 2002). To choose the morphological competitors, we first obtained an estimation of the composition of the community based on our field data. We filtered the list of species by passerine species with at least five total occurrences throughout the

gradient. We then calculated the average nearest neighbor distances among species, using six morphological measurements (beak length, beak width, beak depth, wing chord, tail length, and tarsus length) that were obtained from our measured individuals. Morphological data was supplemented with measurements available from the AVONET database (Tobias et al., 2022) for species that were recorded in point-count surveys but were either not captured or not measured in mist-net surveys. A species' position in multidimensional morphological space may be used as a measure of their ecological function and niche (James, 1982; Ricklefs & Travis, 1980), so species that are closest together in morphospace are more likely to occupy similar niche spaces and be considered potential competitors. The results of the nearest neighbor analysis were then validated to account for elevational range overlap, habitat use, foraging behavior, and guild specification, based on information available from Pigot et al. (2020), Freile et al. (2022) and detailed foraging observations (Drucker, J.R., unpublished data). Analyses were carried out using the “nndist” function in the R package “spatstat.geom” (Baddeley & Turner, 2005).

To choose the phylogenetic competitor, we identified the closest relative present in the community. Information from published phylogenies was corroborated by inspecting a phylogeny based on the BirdTree project (Jetz, Thomas, Joy, Hartmann, & Mooers, 2012), a major phylogenetic dataset that includes 9993 of the ~10,000 extant bird species. We randomly sampled 10 of the 10,000 available trees based on the Hackett et al. (2008) phylogeny and obtained a 50% majority rule consensus tree in R using the “ape” package (Paradis & Schliep, 2019). When there were two or more very close relatives, we determined the genetic distance between the focal species and candidate competitor species. Genetic distances were obtained based on an uncorrected pairwise distance matrix of ND2 (NADH dehydrogenase subunit 2) gene sequences downloaded from GenBank (<https://www.ncbi.nlm.nih.gov>) and aligned on

Clustal X (Larkin et al., 2007). The distance matrix was obtained with PAUP 4.0 b10 (Swofford, 2001). To choose the closest competitor, we picked the candidate species that showed the smallest uncorrected pairwise distance to the focal species.

Both for mist-net and point count data we fitted a set of 18 covariate combinations to estimate the abundance function. Final N -mixture models were selected based on the Akaike Information Criterion (AIC). Model fit and overdispersion (\hat{c}) were assessed through Pearson's chi-square Goodness-of-fit testing, using 1000 parametric bootstrap simulations with the function "Nmix.gof.test" available in the "AICcmodavg" R package (Mazerolle, 2023). When $\hat{c} > 1$, which suggested data overdispersion, we adjusted model selection using quasi-AIC (QAIC) and adjusted the SEs of model parameter estimates accordingly. Predicted abundance response curves were obtained from models that converged. Hereafter, we use the term "best model" as that model with $\Delta AIC \geq 2$ relative to the next model (Burnham & Anderson, 2004); "best set of models" as those falling within $\Delta AIC \leq 2$ and "top-ranked model" as the single model with the smallest AIC value in the entire model set (even when it showed a $\Delta AIC < 2$ from other models).

3. RESULTS

We sampled the montane forests of the Chocó slope of the Northern Ecuadorian Andes along an extensive elevational gradient using mist-nets and point count surveys. We documented 135 species via mist-netting and 241 species through point counts. We filtered our dataset to include only passerine species detected in at least eight sites throughout the gradient and whose elevational ranges were contained within the extent of our sampling. We selected and analyzed a set of 14 species from each dataset, of which three (*Myiothlypis coronata*, *Diglossa cyanea*, and

Henicorhina leucophrys) were analyzed using data from both datasets, for a resulting analysis comprising 25 species of forest birds.

3.1. Shape of the abundance curve

We tested the shape of the abundance distributions of 25 understory passerine species. We were able to fit the full set of five HOF models for eight species detected on point-counts (hereafter “point count species”) and three species detected with mist-nets (hereafter “mist-net species”) (Table 3; Figure 2). Among these species, we found a diversity of shapes in the abundance distributions. From the eight-point count species, two had the symmetric model as the best fit for the shape of their abundance distribution: *Grallaria saturata* (Figure 2d) and *Myiothlypis coronata* (Figure 2g). In both cases, the skewed model was within $\Delta \text{BIC} \leq 2$ of the symmetric model. The modeled abundance peak for *Grallaria saturata* with the symmetric model was skewed towards the upper third of the range (0.73) (Table 3). For *Myiothlypis coronata*, the position of the peak of modeled abundance (0.35) corresponded with the central portion of the range (0.33–0.66). For one point count species, *Arremon assimilis* (Figure 2a), the best model was skewed, with the modeled peak of abundance at position 0.68, in the threshold between the central and upper sections of the scaled elevational range. Three species had the flat model as the best fit: *Atlapetes latinuchus* (Figure 2b), *Myioborus melanocephalus* (Figure 2f), and *Ochthoeca diadema* (Figure 2h).

The shapes of the abundance distributions of two species, *Diglossa cyanea* and *Henicorhina leucophrys*, were analyzed in both mist-net and point count data. For *Diglossa cyanea*, the best model for mist-net data was skewed (Figure 3a), with a modeled peak of abundance at 0.27 in the lower section of the range, while the monotonic model was a better fit for the point count

data (Figure 3b), with abundance that peaked at the upper elevational limit of the range. In both cases, the best models had $\Delta \text{BIC} > 2$ relative to the next model. The shapes of the abundance distribution of *Henicorhina leucophrys* were best described by a monotonic model for mist-net data (Figure 3c), with the flat model within $\Delta \text{BIC} < 2$, and the flat model for point count data (Figure 3d). The remaining mist-net species, *Syndactyla subalaris*, was best fit by the flat model (Figure 2k).

3.2. Predictors of the abundance function

We also modeled abundance by testing various combinations of parameters using N -mixture models. Our global models passed the GOF test in 93% of all model-fitting tests, where $P = 0.051\text{--}0.948$ in 26 of 28 models that included 25 species, three of which had data from mist-nets and point counts (*Myiothlypis coronata*, *Diglossa cyanea*, and *Henicorhina leucophrys*). Two out of these 25 species showed a significant effect of the studied parameters on the abundance function, as follows. For *Masius chrysopterus* (mist-nets), the most complex model received substantial support ($\Delta \text{AIC} > 2$) relative to the next model in the entire model candidate set, and the two predictors were statistically significant: “Distance to mid-elevation ($P = 0.00002$) + Population Gravity Index ($P = 0.000003$)”, with an AIC weight of 0.59. After adjusted QAIC selection ($\hat{c} = 1.76$), the model remained as the top-ranked (QAIC weight = 0.38). Model parameter estimates, Standard Errors (*SEs*), *P* values, and QAIC statistics are summarized in Table 4. With this top-ranked model, we obtained predicted abundance responses to each of the two parameters and plotted the predicted abundance estimates over the range of values observed for each predictor (Figure 4). The trends for “Distance to mid-elevation” and “PGI” were consistent in model-averaged predictions (calculated from the models in the best-set of models), with a negative effect of both parameters on the estimates of abundance (not shown).

For *Diglossa cyanea* (mist-nets), the top-ranked model (AIC weight = 0.28) included the single significant parameter of “Distance to mid-elevation” ($P = 0.003$), which was also significant in all models including this parameter (Table 5). Three of the four models including “Distance to mid-elevation” as a covariate were ranked in the best set of models ($\Delta \text{AIC} < 2$). The model remained as the top-ranked model when adjusted for moderate overdispersion ($\hat{c} = 1.39$) using QAIC and tested in the second order QAICc model selection. Predicted abundance in response to “Distance to mid-elevation” is shown in Figure 5a; the negative effect of this predictor on estimated abundance was consistent in model-averaged predictions (Figure 5b).

In the models for the remaining 22 species, we found large *SEs* in the predicted responses of abundance. We thus investigated parameter importance in the best set of models ($\Delta \text{AIC} < 2$) of species in each dataset. Overall, we found that 41% ($n = 9$) of species had the null model among their best set of models, while 59% ($n = 13$) had models with other predictors of abundance in their best set of models.

For mist-net species ($n = 11$), the null model was ranked among the best set of models for two species (Table 6). In the remaining nine species with predictors of abundance, the candidate set of models of five species included the parameter “Presence of competitor”; for the other four species, selected competitors were absent at all sites in the gradient and thus this covariate was not included in their model set. Of these five mist-net species, which had model sets including all combinations of non-mutually exclusive covariates (i.e., elevational distances, presence of competitor, and PGI), we found the following: “Distance to mid-elevation” was included in the best set of models of four out of five species, “Distance to lower limit” in two out of five, “PGI” in five out of five, and “Presence of competitor” in five out of the five species. Of the four mist-net species without “Presence of competitor” as an abundance covariate in their model set,

“Distance to mid-elevation” appeared in the best set of models of three out of four, “Distance to lower limit” in two out of four, and “PGI” in four out of the four species (Table 6).

For point count species ($n = 11$), the null model was among the best set of models of seven species. For the remaining four species with other predictors of abundance among their best set of models, two had “Presence of competitor” as a covariate included in their candidate model set. The best set of models of all four point count species included “Distance to mid-elevation”, three had “Distance to lower limit”, and four had “PGI” as parameters of abundance (Table 6). Overall, combining the species from both datasets whose null models were not among the best set of models ($n = 13$), we found that “Distance to mid-elevation” appeared in 11 out 13 (85%), “Distance to lower limit” in seven out of 13 (54%) and “PGI” in all 13 species (Table 6).

The effect of “Distance to mid-elevation” was negative in six out of seven (86%) mist-net species, and in two out of four (50%) point-count species (Table 6). “Distance to lower limit” had a negative effect in all the species which included this parameter among their best set of models (four mist-net species and three point count species). For mist-net species, “Presence of competitor” had a positive effect for two out of five (40%) species, negative for two out of five (40%), and variable for one out of the five species (20%). For point count species, the effect of “Presence of competitor” was negative in one out of two and variable in one out of two species (50%). A variable direction of the effect of a parameter indicates that the sign of the coefficient was not consistent in all models appearing among the best set of models ($\Delta AIC < 2$), (i.e., positive in some models, negative in others).

The effect of “Population Gravity Index” was negative in four out of nine mist-nets species (45%), positive in three out of nine (33%), and variable in two out of nine (22%); whereas for

point count species, two out of four had a positive effect (50%) and two had a negative effect (50%). Given that three species were analyzed in both datasets (*Myiothlypis coronata*, *Diglossa cyanea*, and *Henicorhina leucophrys*) and because their responses were not consistent across the mist-net and point count analyses, they are not included in the calculations of parameter importance above.

4. DISCUSSION

We used mist-net and point count data for 25 passerine species to ask questions about the shape of their abundance distribution along a tropical elevational gradient in northern Ecuador, and the potential drivers of those patterns using Huisman-Olff-Fresco (HOF) and *N*-mixture models, respectively. We found that the shape of the abundance distributions varied by species.

Distributions of abundance peaked in varying areas of the elevational range, and in some cases had no discernible peak. Out of the 25 species, all five HOF models converged for only 11 species, of which two, *Diglossa cyanea* and *Henicorhina leucophrys*, had differing responses across both datasets. Hence, considering only point count species ($n = 8$), we found that only two (25 %) were best fitted to symmetric models, of which only one (*Myiothlypis coronata*) had a modeled peak of abundance that corresponded to the central portion of its range, as predicted by the abundant-centre hypothesis. One species (12.5%) was best described by a skewed distribution towards the upper edge of the elevational distribution, one by an increasing monotonic shape (12.5%) and four species' elevational abundance (50 %) were best described by flat shapes (no change on abundance along the gradient). We did not find support for the abundant-centre hypothesis based on our analysis of the shapes of the abundance distributions of bird species along the elevational gradient.

Freeman & Beehler (2018) also found limited support for the abundant-centre hypothesis in a tropical elevational gradient in Papua New Guinea, where the abundance distributions of only 40% of species investigated were accurately described by symmetric models. The authors concluded that New Guinean birds have various distributions of abundance along that elevational gradient. The share of species with symmetric distributions of abundance in their study (40%) is considerably higher than in ours (12.5%, if we are conservative given the position of the modeled peaks of abundance). It is worth noting that the Freeman study had more than three times the sampling effort as ours (27517.74 vs 7487.5 net-hours) with more than a 1000 net-hours per site, and that their gradient consists of mainly primary forest in a remote mountain range contained within a single conservation area (Freeman, 2013). Although we sampled within nature reserves, we also sampled along some secondary but frequented roads, so that overall our study area represents a much more fragmented matrix of forest habitat (Noh et al., 2020) in which other factors may be influencing the abundance distributions of birds.

One explanation for the variation in the shapes of the abundance distributions we found has been recently reviewed by Fristoe, Vilela, Brown, & Botero (2023), who propose that “core-abundant thinking” may be a more accurate portrayal of the relationship between species’ abundances and range position. At its most fundamental, the abundant-centre hypothesis assumes that environmental gradients of suitability shape spatial variation of species abundance (Brown, Mehlman, & Stevens, 1995). Despite that intuitive simplicity, given the ecological complexities embedded in many biogeographic regions, deviations from the abundant-centre pattern are more likely to occur in systems with high environmental heterogeneity, as is the case in tropical mountainous areas. Fristoe et al. (2023) propose an abundant core distribution as an explanation for these deviations, where abundance may peak at a core region somewhere within a species’

range, but that does not necessarily correspond to the geographic center. This flexibility may provide a more realistic understanding of how the abundance of species varies across space, and in particular supports our findings for distributions with abundance peaks skewed towards the edges of elevational ranges (Figure 2).

There may be other factors, not considered in this study, that may help explain the diversity in abundance distributions along elevational gradients. Parameters such as vegetation structure, habitat heterogeneity, and resource availability (Jankowski, Merkord, et al., 2013) may play different roles on the elevational distribution patterns of birds at different portions of their range. Also, at lower elevations where climatic conditions are less harsh and where resources may be more abundant, biotic factors such as competition, predation, and host-parasite interactions may influence spatial patterns more strongly (Jankowski, Londoño, et al., 2013). At higher-stress portions of the range that correspond to higher elevations, abiotic drivers may have a more pronounced effect in community and abundance patterns (MacArthur, 1972). This idea, that climatic conditions constrain the upper sections of species' distributions and biotic interactions constrain the lower portions (Louthan et al., 2015) may be one explanation for the variation in abundance patterns that we have found in this study, that may also result from variations in the intensity of these pressures along the gradient and among species.

A previous study in an elevational gradient in the southern Andes of Ecuador found that climatic conditions (high precipitation at low and mid elevations, and low temperatures at high elevations) rather than overall resource (flower, fruit, and invertebrate) availability were the main predictors of spatio-temporal patterns of bird species richness, evenness, and abundance (Santillán et al., 2018). While they did not find significant changes in overall bird abundance along the gradient, they found temporal fluctuations related to seasonal variation, where bird

abundances increased consistently at all elevations in the driest season. This pattern was attributed to the corresponding decrease in bird evenness during the driest season, along with a strong association between species richness and abundance. Additionally, seasonal movements of birds across portions of the gradient may contribute to these variations (Terborgh, 1985).

Finally, the guild-specific responses in bird communities along elevational gradients may be another reason for the variation in the shapes of the abundance distributions we encountered. The differential effects of elevation (Santillán et al., 2020) and vegetation structure and tree composition (Jankowski, Merkord, et al., 2013) on insectivore and frugivore richness in Andean bird communities are indicators of the complex and idiosyncratic responses that are mediated by the specialized needs of different guilds and even among species within the same guild.

We recognize that our sample size may be limited, and that fitting complex models for species captured or detected at fewer sites along the gradient may not provide an accurate depiction of their underlying abundance patterns. Similarly, species with lower overall relative abundances may be more difficult to detect, and so uncovering consistent elevational patterns becomes more challenging. While we took measures to ensure species' elevational breadths were contained within the extent of our sampling, it is likely that more information is needed about the true elevational limits of the species analyzed in this study. For instance, when we analyzed the shapes of abundance distributions for two species with both mist-net and point count data (*Henicorhina leucophrys* and *Diglossa cyanea*), we found differing responses in the best model that described their distributions for each dataset (Table 3, Figure 3). In the case of *Henicorhina leucophrys*, we found a plausible explanation for this difference. According to the most recently published list of birds for Ecuador (Freile et al., 2022), the lower elevational limit for this species is 1500 m a.s.l., with occurrences of extra-limital records (at 100, 400–500, 500–750, and 3200

m a.s.l.). A comparison with our mist-net data showed that this species was also captured at 960 m a.s.l. and, thus, our survey for point counts (1350–3800 m a.s.l.) does not cover the full extent of this species' elevational breadth. It is probable that expanding this dataset with more extensive field sampling to increase both the sample size and the elevations covered in the gradient will yield more precise results about the elevational patterns of abundance and the factors driving them.

We also found that all four predictors of abundance appeared in the best set of models of most of the species we analyzed. The prevalence of all these parameters among the best set of models are gauges of the complexity of the mechanisms that underlie richness and abundance patterns in Andean mountains, including the effects of biotic interactions, anthropogenic pressure, and the indirect and direct effects of elevation.

We expected “Presence of competitor” to have a negative effect on the abundance of our focal species (Elsen, Tingley, Kalyanaraman, Ramesh, & Wilcove, 2017), but we found this trend in only three out of the seven species which included that parameter among their best set of models. The remaining species either had positive ($n = 2$) or variable effects ($n = 2$) for “Presence of competitor”. We purposefully defined potential competitors as those that may coexist in sympatry with our focal species, but these varying responses among species require a more thorough assessment of competition among bird species. The dynamics of interspecific competition in shaping distributions of bird species across elevational gradients have been rigorously studied (Burner et al., 2020; Freeman et al., 2022; Terborgh & Weske, 1975). These efforts have provided a more nuanced understanding of how interactions among closely related species may drive elevational replacements and “abundant edge” patterns (Diamond, 1973). Because competition is difficult to quantify, these studies often consist of field experiments that

assess the responses to song playback as proxies for interspecific aggression (Freeman, Class Freeman, & Hochachka, 2016) or use congener species richness to assess how competition may shape bird distributions (Laube, Graham, & Böhning-Gaese, 2013). Our measure of interspecific competition, which considers only the presence or absence of one (or two) competitors for each of our focal species, may be an over-simplification of the subtleties of antagonistic biotic interactions among bird species (Jankowski et al., 2012).

Furthermore, in this study we have included the presence or absence of the closest morphological or phylogenetic competitor for each species analyzed as a predictor of abundance, but testing how the abundance and not merely the occurrence of competitors affects overall abundance distributions may reveal underlying community patterns in this slope of the Ecuadorian Andes. To do this we would need to model the abundance of competitors accounting only for detectability without any abundance covariates, and then include the modeled abundance estimate of the competitors at each site as a predictor of abundance for our focal species (Elsen et al., 2017). Another approach to assess the abundance distributions of the bird assemblages in this gradient may be community modelling, as recently studied by Céspedes Arias, Wilson, & Bayly (2022), who found evidence for a mid-elevation abundance peak in the community response of migratory bird species in the Colombian Andes. Interestingly, this study also factored in the relative influence of elevation, land, and forest cover types at the local and landscape scales, and abiotic conditions such as precipitation seasonality for an exhaustive assessment of parameters shaping abundance distributions along a neotropical elevation gradient.

Our results regarding the effects of anthropogenic pressure may be explained through the differences in sensitivity to disturbance of various bird species. We generally expected human disturbance, included in our models as Population Gravity Index, to negatively affect abundance,

especially for forest-interior birds. Nevertheless, we also expected a positive effect for species that may be successful in more disturbed sites, such as forest edges, pastures, gardens, or orchards, as is the case for some species in the *Thraupidae* family (O’Dea & Whittaker, 2007). For instance, we found a positive effect of PGI for *Diglossa cyanea* (Tables 2 and 3), a flowerpiercer that we captured inside forests but that is also found in forest edges and open landscapes (Rodewald & Rodewald, 2003). This result is consistent with a study in a mosaic of the mid-montane cloud forests of our gradient (Becker, Loughin, & Santander, 2008) where the authors sampled the bird community at various habitats including forest interior, edge, pasture, and forest fragments to identify forest-obligate birds. They found that *Diglossa cyanea* had higher capture rates in pastures and forest fragments compared to forest interior sites. The study points out other species that are instead sensitive to forest loss, including *Myadestes ralloides*, for which we correspondingly found a negative effect of PGI (Table 6). Two other species from that study that also showed high sensitivity to forest loss were *Mionectes striaticollis* and *Myiophobus flavicans*. Contrastingly, we found a positive effect of PGI on abundance for both species (Table 6). However, another result that was consistent with our predictions on forest interior birds was the negative effect of PGI on the abundance of *Masius chrysopterus* (Table 6). This response concurs with previous studies on the resilience and habitat preferences of Andean montane forest birds (O’Dea & Whittaker, 2007), showing that *Masius chrysopterus* prefers forest interiors and may be limited in its ability to use other habitats.

The effects of anthropogenic disturbance on bird distributions are complex (Fontúrbel, Orellana, Rodríguez-Gómez, Tabilo, & Castaño-Villa, 2021; Tien, Soh, Sodhi, Lian, & Lim, 2005). A study in the Colombian Andes (Mills et al., 2022) found an interspecific sensitivity gradient in occupancy response to disturbance in the eastern cordillera, where species at lower

elevations were more sensitive to habitat loss than those at higher elevations. The authors suggest that these differences may be caused by more persistent selection pressures on high altitude species, which may be more adapted to habitat configurations that naturally include aspects associated with disturbance, such as reduced canopy cover, fragmentation, and loss of structural complexity. Similarly, Newbold et al. (2014) found that human population density negatively and significantly affected the probability of occupancy of forest-specialist and narrow-ranged birds in a global model including more than 3000 taxa and more than 1000 bird species in tropical and subtropical regions. While our measure of anthropogenic disturbance accounts for both the effects of population size and the proximity of the closest populated place to each of our study sites, it is likely that a finer scale in our variable is required to override the spatial clustering of our field sites, given that the closest populated place to each site was the same for many of the sites located in each geographic sampling area. This will also provide more certainty around the estimates of abundance based on this predictor.

Conclusions

In this study we investigated the abundance distributions of forest passerine species and their driving factors along an elevational gradient in the northwestern Ecuadorian Andes, one of the most unique and biodiverse geographic regions (Myers et al., 2000). We show that the elevational distribution of bird abundance in these tropical mountain forests varies among species, and that no single parameter predicts local spatial patterns throughout the gradient. Our results point towards the complex and multifaceted interplay of ecological factors that shape species' distributions in the Andes, and they reinforce the need to develop more effective conservation strategies that are imperative to preserve mountain habitats in the face of climate change and persistent anthropogenic pressure (Freeman et al., 2018; Roy et al., 2018). More data

is required to detect nuanced elevational patterns of abundance and to obtain finer assessments of the ways in which biotic and abiotic parameters are shaping abundance distributions in this local tropical mountain system.

Tables

Table 1. Names, geographical location, and elevational ranges of each study site where mist-net sampling was carried out between 2021 and 2022.

| Location | Province | Latitude | Longitude | Elevation (m a.s.l) |
|---|-----------------|-----------------|------------------|----------------------------|
| Yanacocha Biological Reserve (YNC) | Pichincha | -0.1117394 | -78.5848561 | 3400–3800 |
| El Pahuma Orchid Reserve (PM) | Pichincha | 0.0109003 | -78.6389355 | 2550–2700 |
| Bellavista Cloud Forest Reserve (BV) | Pichincha | -0.0159828 | -78.6808559 | 2000–2400 |
| Intillacta Reserve (INT) | Pichincha | 0.0496791 | -78.7180884 | 1820–1860 |
| Un Poco del Chocó (UPDC) | Pichincha | 0.0529950 | -78.8422320 | 1000–1200 |
| Mashpi Reserve/Pachijal | Pichincha | 0.1659010 | -78.8776050 | 786–950 |

Table 2. Transect coordinates and elevations where point count surveys were carried out in the northwestern slope of the Ecuadorian Andes in July and August 2022 (47 points in total)

| Transect | Start point (latitude, longitude) | Elevation | End point (latitude, longitude) | Elevation | Number of point counts |
|---|--|------------------|--|------------------|---------------------------------------|
| Mindo Road | -0.046417, -78.774912 | 1350 | -0.036381, -78.763184, | 1500 | 4 |
| Tandayapa Valley | -0.032102, -78.76027 | 1550 | -0.020713, -78.685011 | 2350 | 17 |
| Puluhua Geobotanical Reserve | 0.03963, -78.505067 | 2450 | 0.02128,- 78.503247 | 3050 | 13 |
| Yanacocha Biological Reserve | -0.136919, -78.595753 | 3200 | -0.12267,- 78.585154 | 3800 | 13 |

Table 3. Summary of species used to analyze the shape of their abundance distribution in the elevational gradient. We specify the sampling method (PC = point counts, MN = mist-nets), total number of individuals detected, the number of sites with detections, their elevational limits and breadth, the elevation with highest abundance, the position of the modeled abundance peak using the best fit model, and the HOF models with the best fit (as well as Δ BIC <2).

| Species | Method | Individuals detected | Sites with detections | Lower limit (m) | Upper limit (m) | Elevational breadth | Elevation of highest abundance | Scaled elevation of highest abundance | Position of modeled abundance peak | Best HOF model (and Δ BIC <2) |
|---------------------------------|--------|----------------------|-----------------------|-----------------|-----------------|---------------------|--------------------------------|---------------------------------------|------------------------------------|--------------------------------------|
| <i>Arremon assimilis</i> | PC | 38 | 17 | 2500 | 3750 | 1250 | 3250 | 0.60 | 0.68 | Skewed (symmetric) |
| <i>Atlapetes latinuchus</i> | PC | 41 | 16 | 2650 | 3800 | 1150 | 3600 | 0.83 | Flat | Flat |
| <i>Diglossa cyanea</i> | MN | 41 | 12 | 2105 | 3789 | 1684 | 2566 | 0.27 | 0.27 | Skewed |
| <i>Diglossa cyanea</i> | PC | 59 | 24 | 1850 | 3600 | 1750 | 3500 | 0.94 | 1 | Monotonic |
| <i>Grallaria saturata</i> | PC | 22 | 11 | 3050 | 3800 | 750 | 3600 | 0.73 | 0.73 | Symmetric (skewed) |
| <i>Henicorhina leucophrys</i> | MN | 33 | 12 | 960 | 2620 | 1660 | 2364 | 0.85 | 1 | Monotonic (flat) |
| <i>Henicorhina leucophrys</i> | PC | 82 | 21 | 1350 | 3350 | 2000 | 2150 | 0.40 | Flat | Flat |
| <i>Myioborus melanocephalus</i> | PC | 39 | 15 | 2450 | 3800 | 1350 | 3500 | 0.78 | Flat | Flat (symmetric) |
| <i>Myiothlypis coronata</i> | PC | 93 | 24 | 1750 | 3050 | 1300 | 2000 | 0.19 | 0.35 | Symmetric (skewed) |
| <i>Ochthoeca diadema</i> | PC | 28 | 13 | 2100 | 3250 | 1150 | 2350 | 0.22 | Flat | Flat (skewed) |
| <i>Syndactyla subalaris</i> | MN | 15 | 8 | 1037 | 2376 | 1339 | 1866 | 0.62 | Flat | Flat (symmetric) |

Table 4. Quasi AIC model selection results, estimated parameter coefficients, SEs, and P values for all models fitted to the mist-net data of *Masius chrysopterus*. Significant P values are italicized and in bold. GOF P value for most complex model (*) = 0.051, SEs adjusted for $\hat{c} = 1.76$. Missing SEs were not estimated.

| Models | QAIC | Δ QAIC | QAIC weight | Distance to mid-elevation | Distance to lower limit | PGI |
|---|-------------|---------------------------------|--------------------|---|---|--|
| Distance to mid-elevation + PGI* | 57.40 | 0.00 | 0.38 | -0.011 \pm 0.003 <i>(0.00002)</i> | | -5.862 \pm 1.663 <i>(0.000003)</i> |
| PGI | 58.05 | 0.65 | 0.27 | | | -2.136 \pm 1.04 <i>(0.006)</i> |
| Distance to lower limit + PGI | 58.87 | 1.47 | 0.18 | | -0.002 | -1.443 |
| Distance to lower limit | 59.58 | 2.18 | 0.13 | | -0.002 \pm 0.002 <i>(0.044)</i> | |
| Null | 63.23 | 5.84 | 0.02 | | | |
| Distance to mid-elevation | 63.76 | 6.37 | 0.02 | -0.0002 \pm 0.002 <i>(0.862)</i> | | |

Table 5. Quasi AIC model selection results, estimated parameter coefficients, SEs, and P values for all models fitted to the mist-net data of *Diglossa cyanea*. Significant P values are italicized and in bold. GOF P value for global model (*) = 0.138, SEs adjusted for $\hat{c} = 1.39$.

| Model | QAIC | Δ QAIC | QAIC weight | Distance to mid-elevation | Distance to lower limit | PGI | Competitor |
|---|-------|---------------|-------------|--------------------------------------|---------------------------------|------------------------------|-------------------------------|
| Distance to mid-elevation | 62.90 | 0.00 | 0.28 | -0.003 \pm 0.001 <i>(0.003)</i> | | | |
| PGI | 63.59 | 0.69 | 0.20 | | | 7.764 \pm 4.676 (0.05) | |
| Distance to mid-elevation + Phylo competitor | 64.21 | 1.31 | 0.14 | -0.004 \pm 0.002 <i>(0.01)</i> | | | 0.915 \pm 0.911 (0.236) |
| Distance to mid-elevation + PGI | 64.87 | 1.97 | 0.10 | -0.003 \pm 0.001 <i>(0.02)</i> | | 0.079 \pm 7.243 (0.99) | |
| PGI + Phylo competitor | 65.52 | 2.62 | 0.08 | | | | 0.147 \pm 0.557 (0.755) |
| Phylo competitor | 65.70 | 2.80 | 0.07 | | | | -0.039 \pm 0.516 (0.929) |
| Distance to mid-elevation + PGI + Phylo competitor* | 66.30 | 3.40 | 0.05 | | | 0.08 \pm 7.938 (0.99) | 0.93 \pm 0.687 (0.110) |
| Distance to lower limit | 66.53 | 3.63 | 0.05 | | -0.0002 \pm 0.0003 (0.326) | | |
| Distance to lower limit + PGI | 68.11 | 5.21 | 0.02 | | -0.0002 \pm 0.0003 (0.344) | 0.887 \pm 5.906 (0.859) | |
| Distance to lower limit + Phylo competitor | 69.20 | 6.30 | 0.01 | | -0.0006 \pm 0.001 (0.530) | | 0.786 \pm 2.144 (0.665) |
| Distance to lower limit + PGI + Phylo competitor | 71.18 | 8.28 | 0.00 | | -0.0007 \pm 0.001 (0.429) | 0.582 \pm 6.634 (0.918) | 0.967 \pm 2.180 (0.601) |
| Null | 74.23 | 11.33 | 0.00 | | | | |

Table 6. Summary of the abundance predictors in N -mixture models appearing in the best set of models (Δ AIC < 2) of 25 bird species. We specify the sampling method (PC = point counts, MN = mist-nets), whether the null model was among the best set of models, and the direction (positive, negative, or variable) of the effect of each predictor of abundance, where applicable. “NA” indicates the predictor was either not included in a species’ candidate model set or not appearing in the best set of models, “Null” that the null model was among the best set of models, and * denotes the parameter was statistically significant ($P < 0.05$) in at least one model in the best set of models. A variable response indicates that the sign of the coefficient was not consistent in all models appearing among the best set of models.

| Scientific name | Method | Null among best set of models | Distance to mid-elevation | Distance to lower limit | PGI | Competitor |
|-----------------------------------|--------|-------------------------------|---------------------------|-------------------------|----------|------------|
| <i>Arremon assimilis</i> | PC | No | — | — | — | NA |
| <i>Arremon brunneinucha</i> | MN | Yes | Null | Null | Null | Null |
| <i>Atlapetes latinuchus</i> | PC | Yes | Null | Null | Null | Null |
| <i>Basileuterus tristriatus</i> | MN | No | — | NA | Variable | — |
| <i>Chlorospingus flavigularis</i> | MN | No | — | — | Variable | NA |
| <i>Chlorospingus semifuscus</i> | MN | No | NA | NA | — | NA |
| <i>Cinnycerthia unirufa</i> | PC | Yes | Null | Null | Null | Null |
| <i>Diglossa cyanea</i> | MN | No | —* | — | + | + |
| <i>Diglossa cyanea</i> | PC | No | NA | NA | + | — |
| <i>Diglossa lafresnayii</i> | PC | Yes | Null | Null | Null | Null |
| <i>Grallaria saturata</i> | PC | Yes | Null | Null | Null | Null |
| <i>Hellmayrea gularis</i> | PC | No | + | — | + | Variable |
| <i>Henicorhina leucophrys</i> | MN | Yes | Null | Null | Null | Null |
| <i>Henicorhina leucophrys</i> | PC | No | NA | NA | — | +* |
| <i>Lepidocolaptes lacrymiger</i> | PC | Yes | Null | Null | Null | Null |
| <i>Masius chrysopterus</i> | MN | No | —* | NA | —* | NA |
| <i>Mionectes striaticollis</i> | MN | No | + | — | + | NA |
| <i>Myadestes ralloides</i> | MN | No | NA | NA | — | Variable |
| <i>Myioborus melanocephalus</i> | PC | No | + | —* | —* | — |
| <i>Myiophobus flavicans</i> | MN | No | — | — | + | + |

| Scientific name | Method | Null among best set of models | Distance to mid-elevation | Distance to lower limit | PGI | Competitor |
|-------------------------------|---------------|--------------------------------------|----------------------------------|--------------------------------|------------|-------------------|
| <i>Myiothlypis coronata</i> | MN | Yes | Null | Null | Null | Null |
| <i>Myiothlypis coronata</i> | PC | No | —* | NA | + | +* |
| <i>Myioatriccus ornatus</i> | MN | Yes | Null | Null | Null | Null |
| <i>Ochthoeca diadema</i> | PC | Yes | Null | Null | Null | Null |
| <i>Premnoplex brunnescens</i> | MN | No | — | NA | + | — |
| <i>Scytalopus latrans</i> | PC | No | — | NA | + | NA |
| <i>Syndactyla subalaris</i> | MN | No | — | — | — | + |
| <i>Vireo leucophrys</i> | PC | Yes | Null | Null | Null | Null |

Figure legends

Figure 1. Map of study area in the northwest slope of the Ecuadorian Andes (c) showing location of mist-nets (a) and point-count surveys (b).

Figure 2. Huisman-Olff-Fresco (HOF) models showing the shape of the abundance distributions of 11 passerine species (eight point count species (a–h) and three mist-net species (i–k)). Best models (blue, solid line) and second-best models ($\Delta \text{BIC} < 2$) (red, dotted line) describing the shape of relative abundance are plotted over the scaled elevation range of each species.

Figure 3. Comparison of the shapes of the abundance distributions of the two species analyzed in both datasets (point counts and mist-nets): *Diglossa cyanea* (a-b) and *Henicorhina leucophrys* (c-d).

Figure 4. Predicted abundance of *Masius chrysopterus* in response to each predictor of abundance appearing in the top-ranked model: “Distance to mid-elevation” (a) and “Population Gravity Index”(b) with 95% confidence intervals shown in gray; predicted abundance is shown over the range of values observed for each predictor.

Figure 5. Predicted abundance of *Diglossa cyanea* in response to the predictor of abundance appearing in the top-ranked model: “Distance to mid-elevation” (a) with 95% confidence intervals; predicted abundance is shown over the range of values observed for the predictor. (b) Shows the model-averaged predicted response of “Distance to mid-elevation”, showing a consistent negative effect on abundance.

Figures

Figure 1.

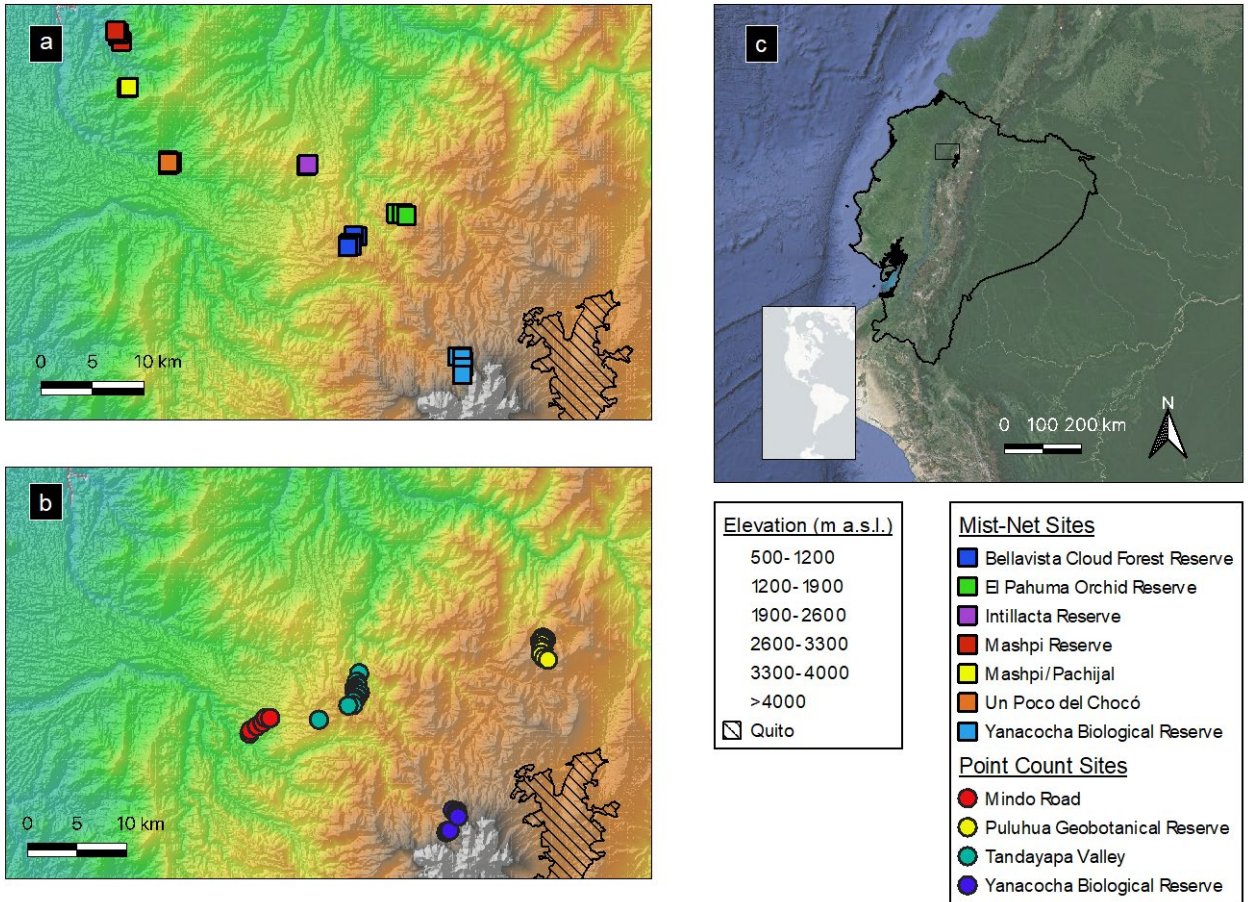


Figure 2.

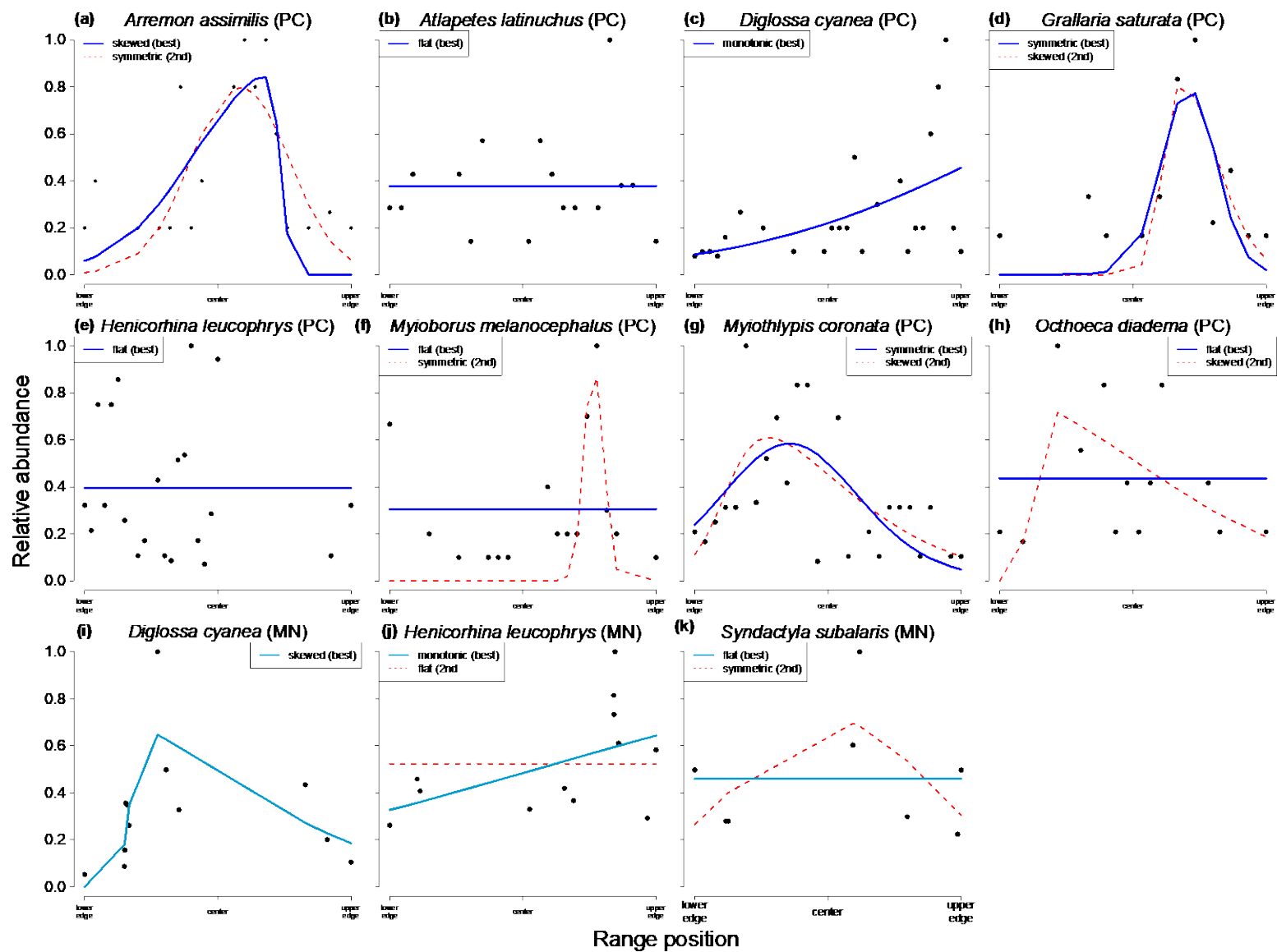


Figure 3.

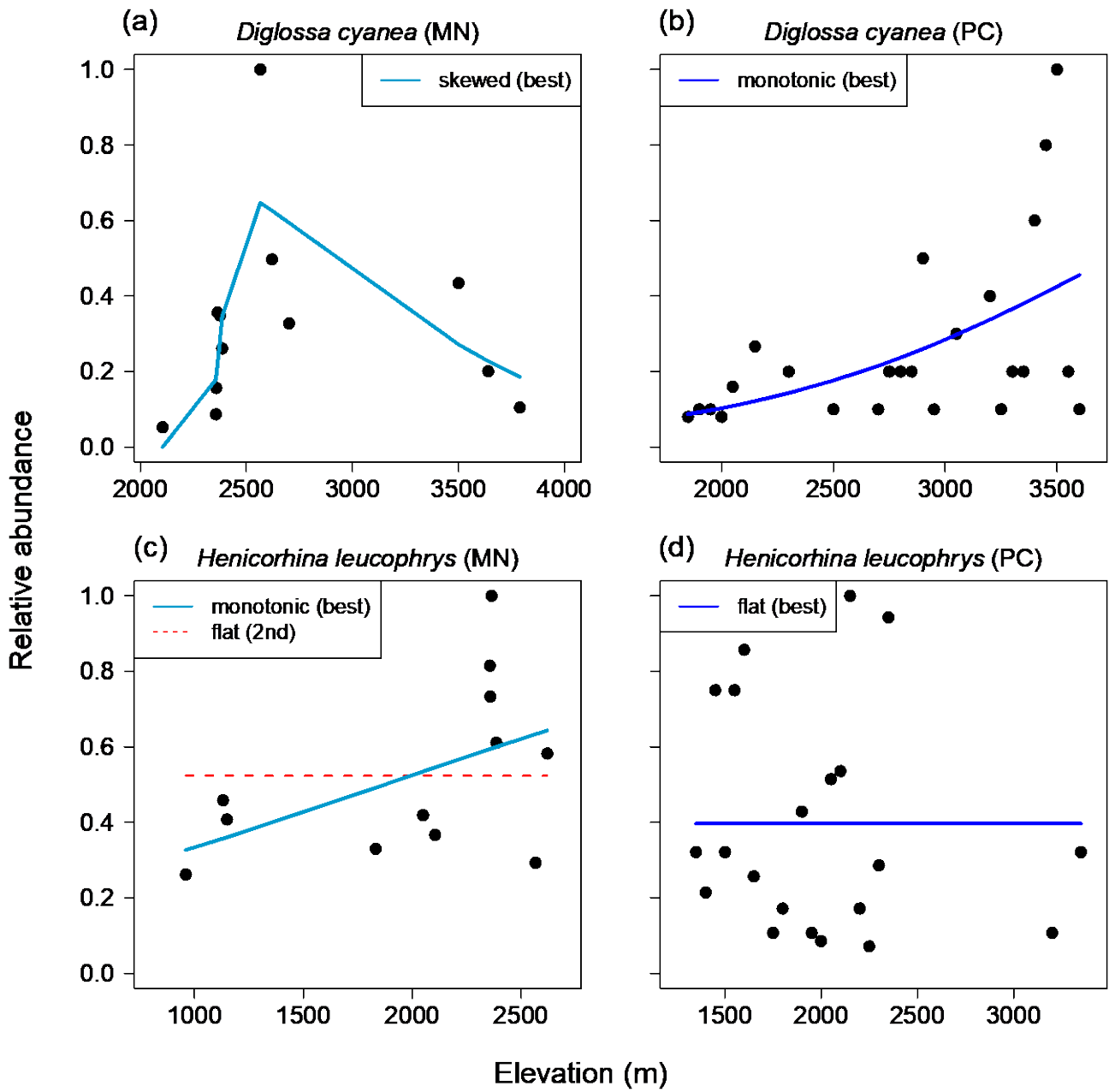
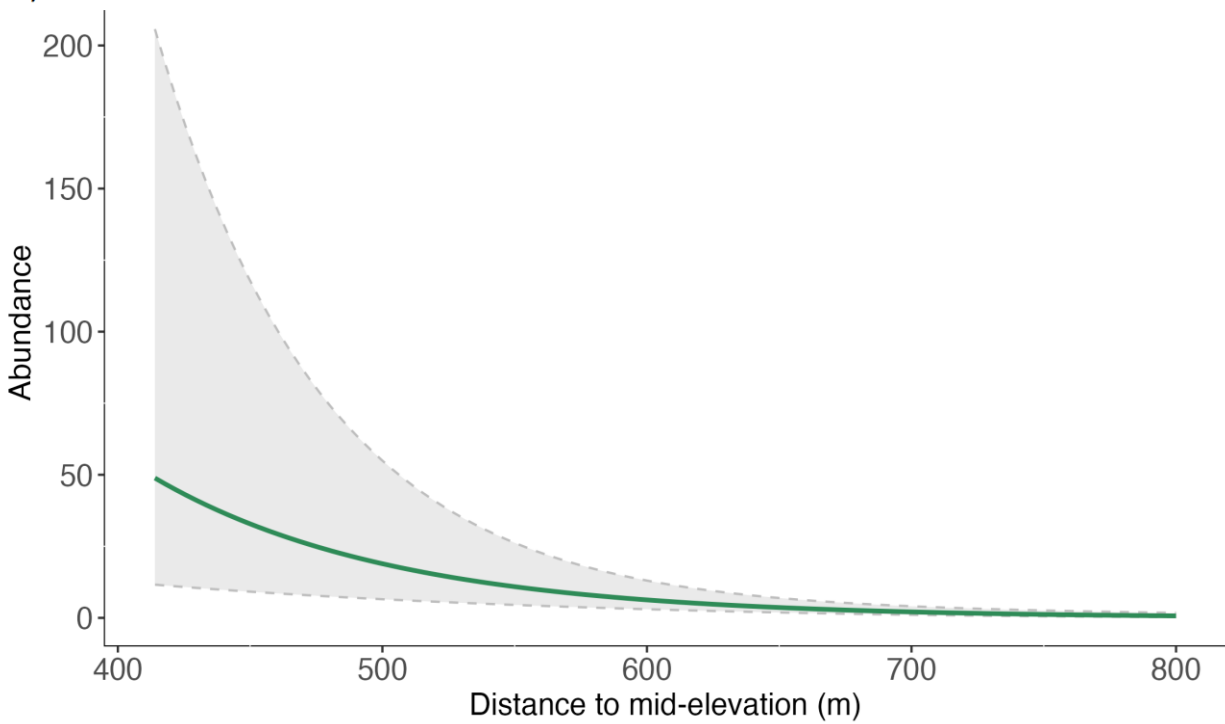


Figure 4.

a) Best model predicted abundance for *Masius chrysopterus* (MN)



b) Best model predicted abundance for *Masius chrysopterus* (MN)

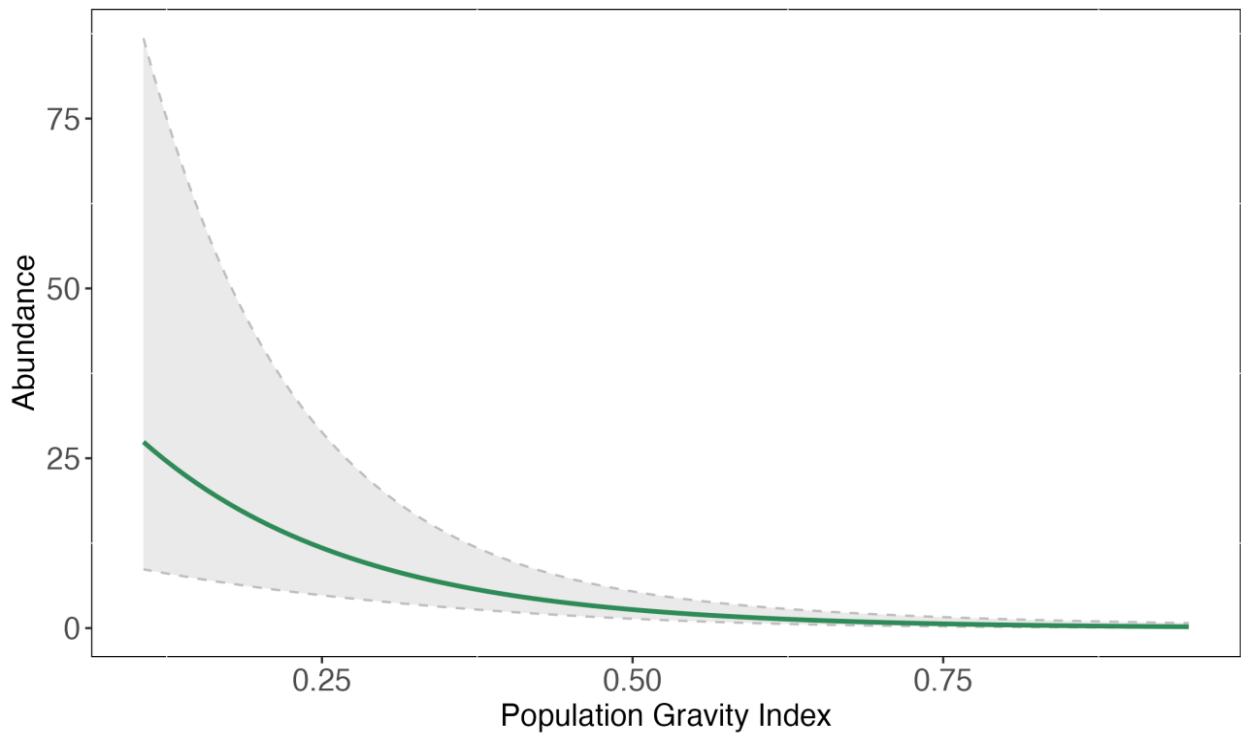
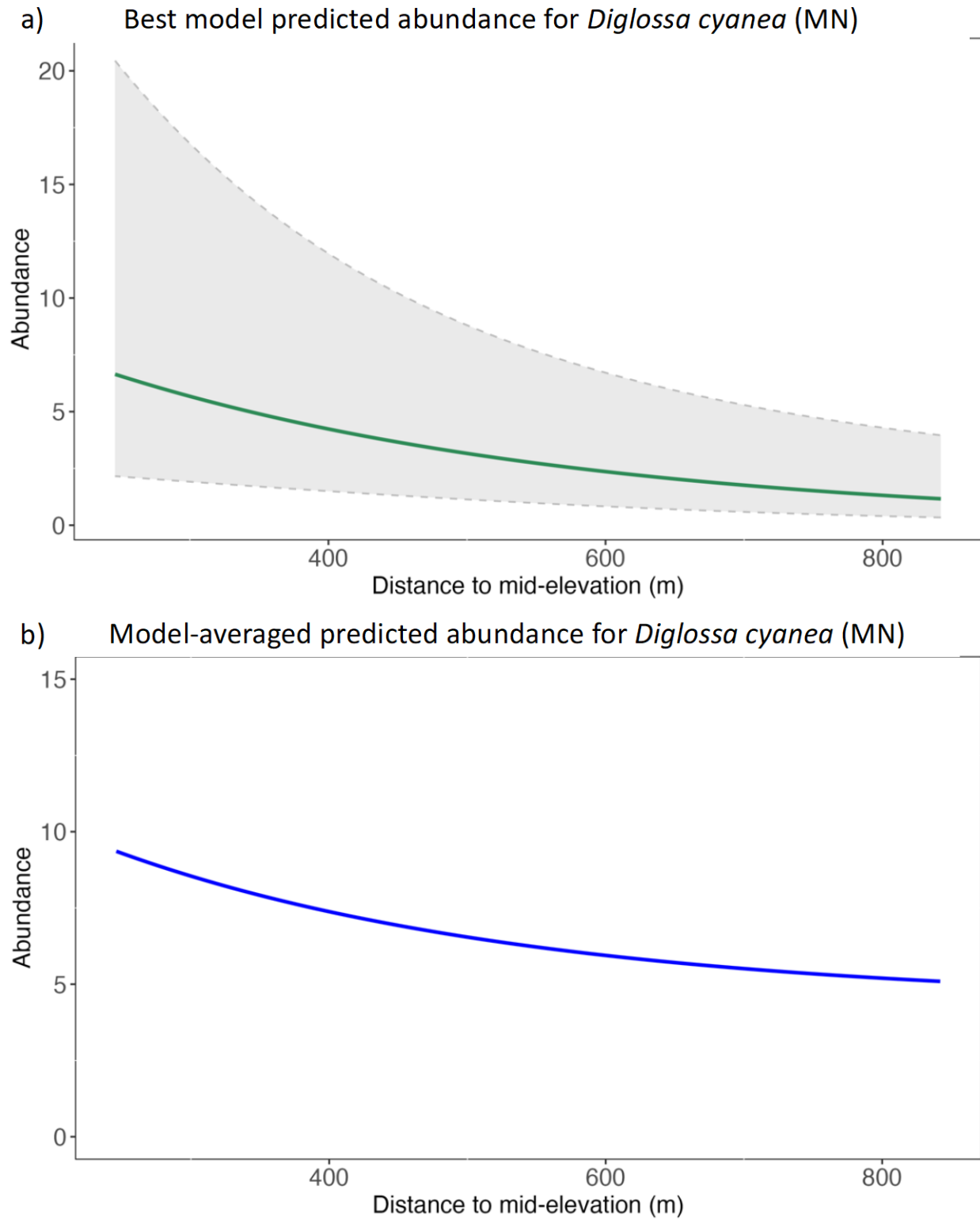


Figure 5.



References

- Baddeley, A., & Turner, R. (2005). spatstat: An R Package for Analyzing Spatial Point Patterns. *Journal of Statistical Software*, 12, 1–42. <https://doi.org/10.18637/JSS.V012.I06>
- Baillie, S. R., Sutherland, W. J., Freeman, S. N., Gregory, R. D., & Paradis, E. (2000). Consequences of large-scale processes for the conservation of bird populations. *Journal of Applied Ecology*, 37(SUPPL. 1), 88–102. <https://doi.org/10.1046/J.1365-2664.2000.00555.X>
- Balmer, O. (2002). Species lists in ecology and conservation: Abundances matter. *Conservation Biology*, 16(4), 1160–1161. <https://doi.org/10.1046/J.1523-1739.2002.01568.X>
- Becker, C. D., Loughin, T. M., & Santander, T. (2008). Identifying forest-obligate birds in tropical moist cloud forest of Andean Ecuador. *Journal of Field Ornithology*, 79(3), 229–244. <https://doi.org/10.1111/J.1557-9263.2008.00184.X>
- Bonaccorso, E., Arzuza, D., Buitrón-Jurado, G., Charpentier, A. L., Juiña, M., Piedrahía, P., & Freile, J. F. (2011). Range extensions and other noteworthy bird records from the Andes of Ecuador. *Bulletin of the British Ornithologists' Club*, Vol 131(4), 261–265.
- Bregman, T. P., Sekercioglu, C. H., & Tobias, J. A. (2014). Global patterns and predictors of bird species responses to forest fragmentation: Implications for ecosystem function and conservation. *Biological Conservation*, 169, 372–383. <https://doi.org/10.1016/J.BIOCON.2013.11.024>
- Brown, J. H. (1984). On the Relationship between Abundance and Distribution of Species. *Am. Nat.*, 124(2), 255–279. Retrieved from <https://www.jstor.org/stable/2461494>
- Brown, J. H., Mehlman, D. W., & Stevens, G. C. (1995). Spatial Variation in Abundance. *Ecology*, 76(7), 2028–2043. <https://doi.org/10.2307/1941678>
- Burner, R. C., Boyce, A. J., Bernasconi, D., Styring, A. R., Shakya, S. B., Boer, C., ... Sheldon, F. H. (2020). Biotic interactions help explain variation in elevational range limits of birds among Bornean mountains. *Journal of Biogeography*, 47(3), 760–771. <https://doi.org/10.1111/JBI.13784>
- Burnham, K. P., & Anderson, D. R. (2004). Multimodel Inference: Understanding AIC and BIC in Model Selection. *Sociological Methods & Research*, 33(2), 261–304. <https://doi.org/10.1177/0049124104268644>
- Calderón-Loor, M., Cuesta, F., Pinto, E., & Gosling, W. D. (2020). Carbon sequestration rates indicate ecosystem recovery following human disturbance in the equatorial Andes. *PLOS ONE*, 15(3), e0230612. <https://doi.org/10.1371/JOURNAL.PONE.0230612>
- Callaghan, C. T., Nakagawa, S., & Cornwell, W. K. (2021). Global abundance estimates for 9,700 bird species. *Proceedings of the National Academy of Sciences of the United States of America*, 118(21), e2023170118. <https://doi.org/https://doi.org/10.1073/pnas.2023170118>
- CEPF. (2001). *Ecosystem Profile Tumbes-Chocó-Magdalena*.
- CEPF. (2021). *Biodiversity Hotspot Tropical Andes: Ecosystem Profile*.
- Céspedes Arias, L. N., Wilson, S., & Bayly, N. J. (2022). Community modeling reveals the importance of elevation and land cover in shaping migratory bird abundance in the Andes. *Ecological Applications*, 32(1). <https://doi.org/10.1002/eap.2481>
- CLIRSEN. (2012). *Watersheds 50K*.
- Cox, C. B., Moore, P. D., & Ladle, R. J. (2016). *Biogeography: an ecological and evolutionary approach* (9th Edition). Wiley-Blackwell.

- Dallas, T. A., Santini, L., Decker, R., & Hastings, A. (2020). Weighing the evidence for the abundant-center hypothesis. In *Biodiversity Informatics* (Vol. 15). <https://doi.org/doi:10.17161/bi.v15i3.11989>
- Dallas, T., Decker, R. R., & Hastings, A. (2017). Species are not most abundant in the centre of their geographic range or climatic niche. *Ecology Letters*, *20*(12), 1526–1533. <https://doi.org/10.1111/ele.12860>
- Danielson, J. J., & Gesch, D. B. (2010). *Global Multi-resolution Terrain Elevation Data 2010 (GMTED2010)*. Retrieved from <https://pubs.usgs.gov/of/2011/1073/pdf/of2011-1073.pdf>
- Diamond, J. M. (1973). Distributional Ecology of New Guinea Birds. *Science*, *179*(4075), 759–769. <https://doi.org/10.1126/SCIENCE.179.4075.759>
- Durães, R., Carrasco, L., Smith, T. B., & Karubian, J. (2013). Effects of forest disturbance and habitat loss on avian communities in a Neotropical biodiversity hotspot. *Biological Conservation*, *166*, 203–211. <https://doi.org/10.1016/J.BIOCON.2013.07.007>
- eBird Basic Dataset. Version: EBD_relDec-2022. (2022). *Cornell Lab of Ornithology*. Ithaca, New York.
- Elsen, P. R., Tingley, M. W., Kalyanaraman, R., Ramesh, K., & Wilcove, D. S. (2017). The role of competition, ecotones, and temperature in the elevational distribution of Himalayan birds. *Ecology*, *98*(2), 337–348. <https://doi.org/10.1002/ECY.1669>
- Elzhov, T. V., Mullen, K. M., Spiess, A.-N., & Bolker, B. (2023, January). *minpack.lm: R Interface to the Levenberg-Marquardt Nonlinear Least-Squares Algorithm Found in MINPACK, Plus Support for Bounds*.
- Esquivel Mattos, A., & Peris, S. (2008). Influence of time of day, duration and number of counts in point count sampling of birds in an atlantic forest of Paraguay. *Ornitologia Neotropical*, *19*(2), 229-242.
- ESRI. (2020). *ArcGIS*. Redlands : ESRI.
- Evans, K. L., Warren, P. H., & Gaston, K. J. (2005). Species-energy relationships at the macroecological scale: a review of the mechanisms. *Biological Reviews of the Cambridge Philosophical Society*, *80*(1), 1–25. <https://doi.org/10.1017/S1464793104006517>
- Fiske, I. J., & Chandler, R. B. (2011). unmarked: An R Package for Fitting Hierarchical Models of Wildlife Occurrence and Abundance. *JSS Journal of Statistical Software*, *43*. <https://doi.org/10.18637/jss.v043.i10>
- Fontúrbel, F. E., Orellana, J. I., Rodríguez-Gómez, G. B., Tabilo, C. A., & Castaño-Villa, G. J. (2021). Habitat disturbance can alter forest understory bird activity patterns: A regional-scale assessment with camera-traps. *Forest Ecology and Management*, *479*, 118618. <https://doi.org/10.1016/j.foreco.2020.118618>
- Freeman, B. (2013). Ornithological survey of the mountains of the Huon Peninsula, Papua New Guinea. *Bulletin of the British Ornithologists' Club*, *144*, 4–18.
- Freeman, B. G., & Beehler, B. M. (2018). Limited support for the “abundant centre” hypothesis in birds along a tropical elevational gradient: implications for the fate of lowland tropical species in a warmer future. *Journal of Biogeography*, *45*(8), 1884–1895. <https://doi.org/10.1111/jbi.13370>
- Freeman, B. G., Class Freeman, A. M., & Hochachka, W. M. (2016). Asymmetric interspecific aggression in New Guinean songbirds that replace one another along an elevational gradient. *Ibis*, *158*(4), 726–737. <https://doi.org/10.1111/IBI.12384>
- Freeman, B. G., Scholer, M. N., Ruiz-Gutierrez, V., & Fitzpatrick, J. W. (2018). Climate change causes upslope shifts and mountaintop extirpations in a tropical bird community.

- Proceedings of the National Academy of Sciences of the United States of America*, 115(47), 11982–11987. <https://doi.org/10.1073/pnas.1804224115>
- Freeman, B. G., Strimas-Mackey, M., & Miller, E. T. (2022). Interspecific competition limits bird species' ranges in tropical mountains. *Science*, 377(6604), 416–420. <https://doi.org/10.1126/science.abl7242>
- Freile, J. F., Ahlman, R., Brinkhuizen, D. M., Greenfield, P. J., Solano-Ugalde, A., Navarrete, L., & Ridgely, R. S. (2013). Rare birds in Ecuador: first annual report of the Committee of Ecuadorian Records in Ornithology (CERO). *Avances*, 5(2), B24–B41. Retrieved from <https://revistas.usfq.edu.ec/index.php/avances/article/view/135/137>
- Freile, J. F., Brinkhuizen, D. M., Greenfield, P. J., Lysinger, M., Navarrete, L., Nilsson, J., ... Boyla, K. A. (2022). *Lista de las aves del Ecuador/Checklist of the birds of Ecuador*. Retrieved from <https://ceroecuador.wordpress.com/>
- Freile, J. F., Solano-Ugalde, A., Brinkhuizen, D. M., Greenfield, P. J., Lysinger, M., Nilsson, J., ... Ridgely, R. S. (2016). Rare Birds in Ecuador: Third Report of the Committee for Ecuadorian Records in Ornithology (CERO). *Revista Ecuatoriana de Ornitología*, 1, 8–27.
- Freile, J., & Restall, R. (2018). *Birds of Ecuador*. London: Bloomsbury Publishing.
- Fristoe, T. S., Vilela, B., Brown, J. H., & Botero, C. A. (2023). Abundant-core thinking clarifies exceptions to the abundant-center distribution pattern. *Ecography*, 2023(2), e06365. <https://doi.org/10.1111/ECOG.06365>
- Gaston, K. J., Blackburn, T. M., & Spicer, J. I. (1998). Rapoport's rule: Time for an epitaph? *Trends in Ecology and Evolution*, 13(2), 70–74. [https://doi.org/10.1016/S0169-5347\(97\)01236-6](https://doi.org/10.1016/S0169-5347(97)01236-6)
- Gaston, K. J., Chown, S. L., & Evans, K. L. (2008). Ecogeographical Rules: Elements of a Synthesis. *Journal of Biogeography*, 35(3), 483–500. <https://doi.org/10.1111/j.1365-2699.2007.01772.x>
- Gilroy, J. J., Edwards, F. A., Medina Uribe, C. A., Haugaasen, T., & Edwards, D. P. (2014). EDITOR'S CHOICE: Surrounding habitats mediate the trade-off between land-sharing and land-sparing agriculture in the tropics. *Journal of Applied Ecology*, 51(5), 1337–1346. <https://doi.org/10.1111/1365-2664.12284>
- Grinnell, J. (1917). *The Niche-Relationships of the California Thrasher*. 34(4), 427–433. <https://doi.org/10.2307/4072271>
- Hackett, S. J., Kimball, R. T., Reddy, S., Bowie, R. C. K., Braun, E. L., Braun, M. J., ... Yuri, T. (2008). A phylogenomic study of birds reveals their evolutionary history. *Science*, 320(5884), 1763–1768. [https://doi.org/DOI: 10.1126/science.1157704](https://doi.org/DOI:10.1126/science.1157704)
- Herzog, S. K., Kessler, M., & Bach, K. (2005). The Elevational Gradient in Andean Bird Species Richness at the Local Scale: A Foothill Peak and a High-Elevation Plateau. *Ecography*, 28(2), 209–222. Retrieved from <http://www.jstor.org/stable/3683816>
- Hoover, E. M., & Giarratani, F. (1971). *An Introduction to Regional Economics*. Retrieved from <https://researchrepository.wvu.edu/rri-web-book>
- Howe, R. W., Davis, G. J., & Mosca, V. (1991). The Demographic Significance of “Sink” Populations. *Biological Conservation*, 57, 239–255. [https://doi.org/10.1016/0006-3207\(91\)90071-G](https://doi.org/10.1016/0006-3207(91)90071-G)
- Huisman, J., Olf, H., & Fresco, L. F. M. (1993). A hierarchical set of models for species response analysis. *Journal of Vegetation Science*, 4(1), 37–46. <https://doi.org/10.2307/3235732>

- Hutchinson, G. E. (1957). Concluding Remarks. *Cold Spring Harbor Lab. Press*, 415–427.
<https://doi.org/doi:10.1101/SQB.1957.022.01.039>
- INEC. (2010). Censo de Población y Vivienda. Retrieved May 23, 2023, from
<https://www.ecuadorencifras.gob.ec/base-de-datos-censo-de-poblacion-y-vivienda/>
- James, F. C. (1982). The ecological morphology of birds: a review. *Annales Zoologici Fennici*, 19(4), 265–275. Retrieved from <http://www.jstor.org/stable/23734869>
- Jankowski, J. E., Graham, C. H., Parra, J. L., Robinson, S. K., Seddon, N., Touchton, J. M., & Tobias, J. A. (2012). THE ROLE OF COMPETITION IN STRUCTURING TROPICAL BIRD COMMUNITIES. *ORNITOLOGIA NEOTROPICAL*, 23, 97–106.
- Jankowski, J. E., Londoño, G. A., Robinson, S. K., & Chappell, M. A. (2013). Exploring the role of physiology and biotic interactions in determining elevational ranges of tropical animals. *Ecography*, 36(1), 1–12. <https://doi.org/10.1111/j.1600-0587.2012.07785.x>
- Jankowski, J. E., Merkord, C. L., Rios, W. F., Cabrera, K. G., Revilla, N. S., & Silman, M. R. (2013). The relationship of tropical bird communities to tree species composition and vegetation structure along an Andean elevational gradient. *Journal of Biogeography*, 40(5), 950–962. <https://doi.org/10.1111/jbi.12041>
- Jankowski, J. E., Robinson, S. K., & Levey, D. J. (2010). Squeezed at the top: Interspecific aggression may constrain elevational ranges in tropical birds. *Ecology*, 91(7), 1877–1884. <https://doi.org/10.1890/09-2063.1>
- Janzen, D. H. (1967). Why Mountain Passes are Higher in the Tropics. *The American Naturalist*, 101(919), 233–249.
- Jetz, W., Thomas, G. H., Joy, J. B., Hartmann, K., & Mooers, A. O. (2012). The global diversity of birds in space and time. *Nature* 2012 491:7424, 491(7424), 444–448. <https://doi.org/10.1038/nature11631>
- Johnston, A., Fink, D., Reynolds, M. D., Hochachka, W. M., Sullivan, B. L., Bruns, N. E., ... Kelling, S. (2015). Abundance models improve spatial and temporal prioritization of conservation resources. *Ecological Applications*, 25(7), 1749–1756. <https://doi.org/10.1890/14-1826.1>
- Jones, J. P. G. (2011). Monitoring species abundance and distribution at the landscape scale. *Journal of Applied Ecology*, 48(1), 9–13. <https://doi.org/10.1111/J.1365-2664.2010.01917.X>
- Kattan, G. H., & Franco, P. (2004). Bird Diversity along Elevational Gradients in the Andes of Colombia: Area and Mass Effects. *Global Ecology and Biogeography*, 13(5), 451–458. Retrieved from <http://www.jstor.org/stable/3697576>
- Kéry, M., Royle, J. A., & Schmid, H. (2005). Modeling Avian Abundance from Replicated Counts Using Binomial Mixture Models. *Ecological Applications*, 15(4), 1450–1461. Retrieved from <http://www.jstor.org/stable/4543451>
- Larkin, M. A., Blackshields, G., Brown, N. P., Chenna, R., Mcgettigan, P. A., McWilliam, H., ... Higgins, D. G. (2007). Clustal W and Clustal X version 2.0. *Bioinformatics (Oxford, England)*, 23(21), 2947–2948. <https://doi.org/10.1093/BIOINFORMATICS/BTM404>
- Laube, I., Graham, C. H., & Böhning-Gaese, K. (2013). Intra-generic species richness and dispersal ability interact to determine geographic ranges of birds. *Global Ecology and Biogeography*, 22(2), 223–232. <https://doi.org/10.1111/J.1466-8238.2012.00796.X>
- Louthan, A. M., Doak, D. F., & Angert, A. L. (2015). Where and When do Species Interactions Set Range Limits? *Trends in Ecology & Evolution*, 30(12), 780–792. <https://doi.org/10.1016/j.tree.2015.09.011>

- MacArthur, R. H. (1972). *Geographical ecology: Patterns in the distribution of species*. Princeton, NJ: Princeton University Press.
- MacArthur, Robert H, & MacArthur, A. T. (1974). On the Use of Mist Nets for Population Studies of Birds. *Proceedings of the National Academy of Sciences of the United States of America*, 71(8), 3230–3233. Retrieved from <http://www.jstor.org/stable/63227>
- Marques, J. T., Ramos Pereira, M. J., Marques, T. A., Santos, C. D., Santana, J., Beja, P., & Palmeirim, J. M. (2013). Optimizing Sampling Design to Deal with Mist-Net Avoidance in Amazonian Birds and Bats. *PLOS ONE*, 8(9), e74505. <https://doi.org/10.1371/JOURNAL.PONE.0074505>
- Martínez-Meyer, E., Díaz-Porras, D., Peterson, A. T., & Yáñez-Arenas, C. (2013). Ecological niche structure and rangewide abundance patterns of species. *Biology Letters*, 9(1). <https://doi.org/10.1098/rsbl.2012.0637>
- Mazerolle, M. (2023). *AICcmodavg: Model selection and multimodel inference based on (Q)AIC(c)*. Retrieved from <https://cran.r-project.org/package=AICcmodavg>
- Mccain, C. M., & Grytnes, J.-A. (2010). Elevational Gradients in Species Richness. In *Encyclopedia of Life Sciences*. <https://doi.org/10.1002/9780470015902.a0022548>
- Mills, S. C., Socolar, J. B., Edwards, F. A., Parra, E., Martínez-Revelo, D. E., Ochoa Quintero, J. M., ... Edwards, D. P. (2022). High sensitivity of tropical forest birds to deforestation at lower altitudes. *Ecology*. <https://doi.org/10.1002/ecy.3867>
- Ministerio del Ambiente del Ecuador. (2013). *Sistema de Clasificación de los Ecosistemas del Ecuador Continental*. Quito.
- Mordecái, R. S., Cooper, R. J., & Justicia, R. (2009). A threshold response to habitat disturbance by forest birds in the Choco Andean corridor, Northwest Ecuador. *Biodiversity and Conservation*, 18(9), 2421–2431. <https://doi.org/10.1007/S10531-009-9599-1/FIGURES/3>
- Myers, N., Mittermeier, R. A., Mittermeier, C. G., da Fonseca, G. A. B., & Kent, J. (2000). Biodiversity hotspots for conservation priorities. *Nature*, 403(6772), 853–858. <https://doi.org/10.1038/35002501>
- Newbold, T., Hudson, L. N., Phillips, H. R. P., Hill, S. L. L., Contu, S., Lysenko, I., ... Purvis, A. (2014). A global model of the response of tropical and sub-tropical forest biodiversity to anthropogenic pressures. *Proceedings of the Royal Society B: Biological Sciences*, 281(1792). <https://doi.org/10.1098/RSPB.2014.1371>
- Newbold, T., Scharlemann, J. P. W., Butchart, S. H. M., Şekercioğlu, Ç. H., Alkemade, R., Booth, H., & Purves, D. W. (2013). Ecological traits affect the response of tropical forest bird species to land-use intensity. *Proceedings of the Royal Society B: Biological Sciences*, 280(1750). <https://doi.org/10.1098/RSPB.2012.2131>
- Noh, J. K., Echeverria, C., Kleemann, J., Koo, H., Fürst, C., & Cuenca, P. (2020). Warning about conservation status of forest ecosystems in tropical Andes: National assessment based on IUCN criteria. *PLOS ONE*, 15(8), e0237877. <https://doi.org/10.1371/JOURNAL.PONE.0237877>
- O’Dea, N., & Whittaker, R. J. (2007). How resilient are Andean montane forest bird communities to habitat degradation? *Biodiversity and Conservation*, 16(4), 1131–1159. <https://doi.org/10.1007/s10531-006-9095-9>
- Osorio-Olvera, L., Yáñez-Arenas, C., Martínez-Meyer, E., & Peterson, A. T. (2020). Relationships between population densities and niche-centroid distances in North American birds. *Ecology Letters*, 23(3), 555–564. <https://doi.org/10.1111/ele.13453>

- Paradis, E., & Schliep, K. (2019). ape 5.0: an environment for modern phylogenetics and evolutionary analyses in R. *Bioinformatics*, *35*(3), 526–528. <https://doi.org/10.1093/BIOINFORMATICS/BTY633>
- Pigot, A. L., Sheard, C., Miller, E. T., Bregman, T. P., Freeman, B. G., Roll, U., ... Tobias, J. A. (2020). Macroevolutionary convergence connects morphological form to ecological function in birds. *Nature Ecology & Evolution* *2020 4:2*, *4*(2), 230–239. <https://doi.org/10.1038/s41559-019-1070-4>
- Polyakov, M., Majumdar, I., & Teeter, L. (2008). Spatial and temporal analysis of the anthropogenic effects on local diversity of forest trees. *Forest Ecology and Management*, *255*(5–6), 1379–1387. <https://doi.org/10.1016/J.FORECO.2007.10.052>
- Pulliam, H. R. (1988). Sources, Sinks, and Population Regulation. *The American Naturalist*, *132*(5). Retrieved from <https://www.jstor.org/stable/2461927>
- Pyle, P. (1997). *Identification Guide to North American Birds, Part I*. Slate Creek Press.
- R Core Team. (2021). *R: A language and environment for statistical computing*. Vienna, Austria: R Foundation for Statistical Computing. Retrieved from <https://www.R-project.org/>.
- Rahbek, C. (1995). The elevational gradient of species richness: a uniform pattern? *Ecography*, *18*(2), 200–205. <https://doi.org/10.1111/j.1600-0587.1995.tb00341.x>
- Rahbek, C. (1997). The relationship among area, elevation, and regional species richness in neotropical birds. *American Naturalist*, *149*(5), 875–902. <https://doi.org/10.1086/286028>
- Remsen, J. V., & Good, D. A. (1996). Misuse of Data from Mist-Net Captures to Assess Relative Abundance in Bird Populations. *The Auk*, *113*(2), 381–398. <https://doi.org/10.2307/4088905>
- Ricklefs, R. E., & Travis, J. (1980). A Morphological Approach to the Study of Avian Community Organization. *The Auk*, *97*(2), 321–338. Retrieved from <http://www.jstor.org/stable/4085704>
- Riegert, J., Chmel, K., Vlček, J., Hrázský, Z., Sedláček, O., Grill, S., ... Hořák, D. (2021). Alarming declines in bird abundance in an Afrotropical global biodiversity hotspot. *Biodiversity and Conservation*, *30*(12), 3385–3408. <https://doi.org/10.1007/s10531-021-02252-1>
- Ríos-Touma, B., Cuesta, F., Rázuri-Gonzales, E., Holzenthal, R., Tapia, A., & Calderón-Loor, M. (2022). Elevational biodiversity gradients in the Neotropics: Perspectives from freshwater caddisflies (Insecta: Trichoptera). *PLOS ONE*, *17*(8), e0272229. <https://doi.org/10.1371/journal.pone.0272229>
- Rodewald, A. D., & Rodewald, P. G. (2003). *Mixed-species bird flocks in primary and regenerating montane forests in Ecuador*.
- Roy, B. A., Zorrilla, M., Endara, L., Thomas, D. C., Vandegrift, R., Rubenstein, J. M., ... Read, M. (2018). New Mining Concessions Could Severely Decrease Biodiversity and Ecosystem Services in Ecuador. *Tropical Conservation Science*, *11*, 194008291878042. <https://doi.org/10.1177/1940082918780427>
- Royle, J. A. (2004). N-Mixture Models for Estimating Population Size from Spatially Replicated Counts. *Biometrics*, *60*(1), 108–115. <https://doi.org/10.1111/J.0006-341X.2004.00142.X>
- Sagarin, R. D., & Gaines, S. D. (2002). The “abundant centre” distribution: to what extent is it a biogeographical rule? *Ecology Letters*, *5*, 137–147. <https://doi.org/https://doi.org/10.1046/j.1461-0248.2002.00297.x>
- Sagarin, R. D., Gaines, S. D., & Gaylord, B. (2006, September). Moving beyond assumptions to understand abundance distributions across the ranges of species. *Trends in Ecology and Evolution*, Vol. 21, pp. 524–530. <https://doi.org/10.1016/j.tree.2006.06.008>

- Santillán, V., Quitián, M., Tinoco, B. A., Zárate, E., Schleuning, M., Böhning-Gaese, K., & Neuschulz, E. L. (2018). Spatio-temporal variation in bird assemblages is associated with fluctuations in temperature and precipitation along a tropical elevational gradient. *PLOS ONE*, *13*(5), e0196179. <https://doi.org/10.1371/journal.pone.0196179>
- Santillán, V., Quitián, M., Tinoco, B. A., Zárate, E., Schleuning, M., Böhning-Gaese, K., & Neuschulz, E. L. (2020). Direct and indirect effects of elevation, climate and vegetation structure on bird communities on a tropical mountain. *Acta Oecologica*, *102*. <https://doi.org/10.1016/j.actao.2019.103500>
- Santini, L., Pironon, S., Maiorano, L., & Thuiller, W. (2018). Addressing common pitfalls does not provide more support to geographical and ecological abundant-centre hypotheses. *Ecography*, *42*(4). <https://doi.org/10.1111/ecog.04027i>
- Sierra, R., Calva, O., & Guevara, A. (2021). *La Deforestación en el Ecuador, 1990-2018. Factores promotores y tendencias recientes*. Quito, Ecuador.
- Stevens, R. D., & Willig, M. R. (2000). Community Structure, Abundance, and Morphology. *Oikos*, *88*(1), 48–56. Retrieved from <http://www.jstor.org/stable/3546394>
- Swofford, D. (2001). *PAUP 4.0 b10*.
- Terborgh, J. (1971). Distribution on Environmental Gradients: Theory and a Preliminary Interpretation of Distributional Patterns in the Avifauna of the Cordillera Vilcabamba, Peru. *Ecology*, *52*(1), 23–40.
- Terborgh, J. (1985). The Role of Ecotones in the Distribution of Andean Birds. *Ecology*, *66*(4), 1237–1246. <https://doi.org/10.2307/1939177>
- Terborgh, J., & Weske, J. S. (1975). The Role of Competition in the Distribution of Andean Birds. *Source: Ecology*, *56*(3), 562–576. <https://doi.org/https://doi.org/10.2307/1935491>
- Teunissen van Manen, M. L., Jansen, B., Cuesta, F., León-Yáñez, S., & Gosling, W. D. (2019). Leaf wax alkane patterns of six tropical montane tree species show species-specific environmental response. *Ecology and Evolution*, *9*(16), 9120–9128. <https://doi.org/10.1002/ece3.5458>
- Tien, M. L., Soh, M. C. K., Sodhi, N., Lian, P. K., & Lim, S. L. H. (2005). Effects of habitat disturbance on mixed species bird flocks in a tropical sub-montane rainforest. *Biological Conservation*, *122*(2), 193–204. <https://doi.org/10.1016/J.BIOCON.2004.07.005>
- Tobias, J. A., Sheard, C., Pigot, A. L., Devenish, A. J. M., Yang, J., Sayol, F., ... Schleuning, M. (2022). AVONET: morphological, ecological and geographical data for all birds. *Ecology Letters*, *25*(3), 581–597. <https://doi.org/10.1111/ELE.13898>
- Webb, C. O., Ackerly, D. D., & McPeck, M. A. (2002). Phylogenies and Community Ecology. *Donoghue Source: Annual Review of Ecology and Systematics*, *33*, 475–505. <https://doi.org/10.1146/annurev.ecolsys.33.010802.150448>

Supplementary Information

Table S1. Summary of model selection using Bayesian Information Criterion (BIC) for the Huisman-Olff-Fresco (HOF) models fitted to abundance data of 14 point count species. Models in bold indicate the best and second-best (Δ BIC < 2) models for species where all five models converged (flat, monotonic, plateau, skewed, and symmetric)

| Species | Model | df | BIC |
|-------------------------------|------------------|----|-------------------|
| <i>Arremon assimilis</i> | flat | 2 | 13.0151565 |
| <i>Arremon assimilis</i> | monotonic | 3 | 15.5200831 |
| <i>Arremon assimilis</i> | plateau | 4 | 16.9638165 |
| <i>Arremon assimilis</i> | symmetric | 4 | 7.06805907 |
| <i>Arremon assimilis</i> | skewed | 5 | 6.6193131 |
| <i>Cinnycerthia unirufa</i> | flat | 2 | 6.17253005 |
| <i>Cinnycerthia unirufa</i> | monotonic | 3 | 7.07727672 |
| <i>Cinnycerthia unirufa</i> | plateau | 4 | 6.60095408 |
| <i>Cinnycerthia unirufa</i> | skewed | 5 | 6.06178149 |
| <i>Diglossa cyanea</i> | flat | 2 | 4.7229132 |
| <i>Diglossa cyanea</i> | monotonic | 3 | 0.74343637 |
| <i>Diglossa cyanea</i> | plateau | 4 | 10.553384 |
| <i>Diglossa cyanea</i> | symmetric | 4 | 3.92149038 |
| <i>Diglossa cyanea</i> | skewed | 5 | 7.0995444 |
| <i>Diglossa lafresnayii</i> | flat | 2 | 8.98550844 |
| <i>Diglossa lafresnayii</i> | monotonic | 3 | 10.7124696 |
| <i>Diglossa lafresnayii</i> | symmetric | 4 | 1.44951324 |
| <i>Diglossa lafresnayii</i> | skewed | 5 | -0.4583661 |
| <i>Grallaria saturata</i> | flat | 2 | 7.82097917 |
| <i>Grallaria saturata</i> | monotonic | 3 | 9.94679451 |
| <i>Grallaria saturata</i> | plateau | 4 | 11.5452763 |
| <i>Grallaria saturata</i> | symmetric | 4 | 4.69161965 |
| <i>Grallaria saturata</i> | skewed | 5 | 6.12486602 |
| <i>Hellmayrea gularis</i> | flat | 2 | 3.4550975 |
| <i>Hellmayrea gularis</i> | monotonic | 3 | 5.82557541 |
| <i>Hellmayrea gularis</i> | symmetric | 4 | 8.22347076 |
| <i>Henicorhina leucophrys</i> | flat | 2 | 14.0424978 |
| <i>Henicorhina leucophrys</i> | monotonic | 3 | 16.627837 |
| <i>Henicorhina leucophrys</i> | plateau | 4 | 19.4871925 |
| <i>Henicorhina leucophrys</i> | symmetric | 4 | 19.6044798 |

| Species | Model | df | BIC |
|----------------------------------|------------------|-----------|-------------------|
| <i>Henicorhina leucophrys</i> | skewed | 5 | 22.5316677 |
| <i>Lepidocolaptes lacrymiger</i> | flat | 2 | -0.0893941 |
| <i>Lepidocolaptes lacrymiger</i> | monotonic | 3 | 1.98633928 |
| <i>Lepidocolaptes lacrymiger</i> | skewed | 5 | 18.8152363 |
| <i>Myioborus melanocephalus</i> | flat | 2 | 8.01152414 |
| <i>Myioborus melanocephalus</i> | monotonic | 3 | 10.654805 |
| <i>Myioborus melanocephalus</i> | plateau | 4 | 12.7611925 |
| <i>Myioborus melanocephalus</i> | symmetric | 4 | 9.75283123 |
| <i>Myioborus melanocephalus</i> | skewed | 5 | 16.0718289 |
| <i>Myiothlypis coronata</i> | flat | 2 | 9.82932854 |
| <i>Myiothlypis coronata</i> | monotonic | 3 | 10.7043538 |
| <i>Myiothlypis coronata</i> | plateau | 4 | 11.09146 |
| <i>Myiothlypis coronata</i> | symmetric | 4 | 5.0682211 |
| <i>Myiothlypis coronata</i> | skewed | 5 | 6.28095122 |
| <i>Ochthoeca diadema</i> | flat | 2 | 8.4278838 |
| <i>Ochthoeca diadema</i> | monotonic | 3 | 10.7396498 |
| <i>Ochthoeca diadema</i> | plateau | 4 | 12.2122741 |
| <i>Ochthoeca diadema</i> | symmetric | 4 | 10.6638871 |
| <i>Ochthoeca diadema</i> | skewed | 5 | 9.63151048 |
| <i>Scytalopus latrans</i> | flat | 2 | 9.59823339 |
| <i>Scytalopus latrans</i> | monotonic | 3 | -0.7148494 |
| <i>Vireo leucophrys</i> | flat | 2 | 8.24252512 |
| <i>Vireo leucophrys</i> | monotonic | 3 | 10.9821468 |
| <i>Vireo leucophrys</i> | plateau | 4 | 12.09827 |
| <i>Vireo leucophrys</i> | symmetric | 4 | 13.6269073 |
| <i>Atlapetes latinuchus</i> | flat | 2 | 0.36882529 |
| <i>Atlapetes latinuchus</i> | monotonic | 3 | 2.94641718 |
| <i>Atlapetes latinuchus</i> | plateau | 4 | 4.45605864 |
| <i>Atlapetes latinuchus</i> | symmetric | 4 | 5.45840524 |
| <i>Atlapetes latinuchus</i> | skewed | 5 | 5.92466818 |

Table S2. Summary of model selection using Bayesian Information Criterion (BIC) for the Huisman-Olff-Fresco (HOF) models fitted to abundance data of 14 mist-net species. Models in bold indicate the best and second-best (Δ BIC < 2) models for species where all five models converged (flat, monotonic, plateau, skewed, and symmetric)

| Species | Model | df | BIC |
|---------------------------------|------------------|----|-------------------|
| <i>Myadestes ralloides</i> | flat | 2 | 7.4220604 |
| <i>Myadestes ralloides</i> | monotonic | 3 | 9.86916954 |
| <i>Myadestes ralloides</i> | symmetric | 4 | 12.5082269 |
| <i>Myadestes ralloides</i> | skewed | 5 | 15.1482939 |
| <i>Arremon_brunneinucha</i> | flat | 2 | 3.28220458 |
| <i>Arremon_brunneinucha</i> | monotonic | 3 | 3.58283051 |
| <i>Arremon_brunneinucha</i> | plateau | 4 | 7.31064276 |
| <i>Arremon_brunneinucha</i> | skewed | 5 | 18.712415 |
| <i>Chlorospingus semifuscus</i> | flat | 2 | 9.06325651 |
| <i>Chlorospingus semifuscus</i> | monotonic | 3 | 9.10842083 |
| <i>Chlorospingus semifuscus</i> | symmetric | 4 | -2.6012285 |
| <i>Chlorospingus semifuscus</i> | skewed | 5 | -0.4242119 |
| <i>Myiophobus flavicans</i> | flat | 2 | 4.13296498 |
| <i>Myiophobus flavicans</i> | monotonic | 3 | 6.12409857 |
| <i>Myiophobus flavicans</i> | symmetric | 4 | 8.30280676 |
| <i>Myiophobus flavicans</i> | skewed | 5 | 10.0001903 |
| <i>Henicorhina leucophrys</i> | flat | 2 | 2.65940792 |
| <i>Henicorhina leucophrys</i> | monotonic | 3 | 1.83141857 |
| <i>Henicorhina leucophrys</i> | plateau | 4 | 7.61850415 |
| <i>Henicorhina leucophrys</i> | symmetric | 4 | 4.28617195 |
| <i>Henicorhina leucophrys</i> | skewed | 5 | 4.98609898 |
| <i>Masius chrysopterus</i> | flat | 2 | 7.81034115 |
| <i>Masius chrysopterus</i> | monotonic | 3 | 8.42939362 |
| <i>Masius chrysopterus</i> | plateau | 4 | 9.31433296 |
| <i>Masius chrysopterus</i> | symmetric | 4 | -10.69292 |
| <i>Syndactyla subalaris</i> | flat | 2 | 4.05190692 |
| <i>Syndactyla subalaris</i> | monotonic | 3 | 6.09164735 |
| <i>Syndactyla subalaris</i> | plateau | 4 | 7.7315854 |
| <i>Syndactyla subalaris</i> | symmetric | 4 | 4.53334484 |
| <i>Syndactyla subalaris</i> | skewed | 5 | 6.56249477 |
| <i>Diglossa cyanea</i> | flat | 2 | 5.35648504 |
| <i>Diglossa cyanea</i> | monotonic | 3 | 7.8239147 |
| <i>Diglossa cyanea</i> | plateau | 4 | 9.21459533 |
| <i>Diglossa cyanea</i> | symmetric | 4 | 3.75974827 |
| <i>Diglossa cyanea</i> | skewed | 5 | 1.72708782 |

| | | | |
|-----------------------------------|-----------|---|------------|
| <i>Myiotriccus ornatus</i> | flat | 2 | 6.20683325 |
| <i>Myiotriccus ornatus</i> | monotonic | 3 | 7.44221666 |
| <i>Myiotriccus ornatus</i> | symmetric | 4 | 10.5985773 |
| <i>Myiothlypis coronata</i> | flat | 2 | 6.97134996 |
| <i>Myiothlypis coronata</i> | monotonic | 3 | 4.00528179 |
| <i>Myiothlypis coronata</i> | symmetric | 4 | 5.09308254 |
| <i>Mionectes striaticollis</i> | flat | 2 | 5.87394259 |
| <i>Mionectes striaticollis</i> | monotonic | 3 | 8.18008945 |
| <i>Mionectes striaticollis</i> | symmetric | 4 | 10.3531533 |
| <i>Mionectes striaticollis</i> | skewed | 5 | 11.4720869 |
| <i>Premnoplex brunnescens</i> | flat | 2 | 10.1229949 |
| <i>Premnoplex brunnescens</i> | monotonic | 3 | 3.15713452 |
| <i>Premnoplex brunnescens</i> | symmetric | 4 | 5.35435911 |
| <i>Basileuterus tristriatus</i> | flat | 2 | 5.18726782 |
| <i>Basileuterus tristriatus</i> | monotonic | 3 | 7.45448486 |
| <i>Basileuterus tristriatus</i> | plateau | 4 | 7.2579145 |
| <i>Basileuterus tristriatus</i> | symmetric | 4 | 5.4404037 |
| <i>Chlorospingus flavigularis</i> | flat | 2 | 7.76989507 |
| <i>Chlorospingus flavigularis</i> | monotonic | 3 | 8.54178744 |
| <i>Chlorospingus flavigularis</i> | symmetric | 4 | 10.5161448 |

Table S3. Locations and sampling effort of 32 sites sampled using mist-nets.

| Location | Site | Latitude | Longitude | GPS elevation | Net-hours |
|---------------------------------|-------------|-----------------|------------------|----------------------|------------------|
| Mashpi Reserve | MSL2 | 0.158737 | -78.883879 | 786 | 282 |
| Mashpi Reserve | MSL1 | 0.163192 | -78.886241 | 838 | 210 |
| Mashpi Reserve | MSL5 | 0.167993 | -78.888668 | 871 | 66 |
| Mashpi Reserve | MSL3 | 0.165271 | -78.885728 | 877 | 78 |
| Mashpi Reserve | MSH3 | 0.118778 | -78.877323 | 938 | 143 |
| Mashpi Reserve | MSH2 | 0.118294 | -78.877883 | 960 | 210 |
| Mashpi Reserve | MSH1 | 0.117725 | -78.878819 | 996 | 190 |
| Un Poco del Chocó | UPDC3 | 0.050233 | -78.843217 | 1002 | 112.5 |
| Un Poco del Chocó | UPDC2 | 0.051005 | -78.843056 | 1037 | 135 |
| Un Poco del Chocó | UPDC4 | 0.05165 | -78.841606 | 1131 | 240 |
| Un Poco del Chocó | UPDC7 | 0.052439 | -78.842666 | 1149 | 270 |
| Un Poco del Chocó | UPDC1 | 0.053777 | -78.842894 | 1193 | 240 |
| Un Poco del Chocó | UPDC6 | 0.052697 | -78.839512 | 1205 | 240 |
| Un Poco del Chocó | UPDC5 | 0.053086 | -78.842316 | 1210 | 315 |
| Intillacta Reserve | INT2 | 0.050692 | -78.72094 | 1832 | 333.5 |
| Intillacta Reserve | INT1 | 0.049893 | -78.722191 | 1866 | 268.25 |
| Bellavista Cloud Forest Reserve | BV2 | -0.011967 | -78.680899 | 2049 | 525 |
| Bellavista Cloud Forest Reserve | BV1 | -0.012276 | -78.678166 | 2105 | 450 |
| Bellavista Cloud Forest Reserve | BV6 | -0.02019 | -78.682939 | 2356 | 270 |
| Bellavista Cloud Forest Reserve | BV3 | -0.018348 | -78.68396 | 2358 | 300 |
| Bellavista Cloud Forest Reserve | BV5 | -0.020441 | -78.686074 | 2364 | 330 |
| Bellavista Cloud Forest Reserve | BV4 | -0.019159 | -78.682813 | 2376 | 270 |
| Bellavista Cloud Forest Reserve | BV7 | -0.021721 | -78.686061 | 2386 | 180 |
| El Pahuma Orchid Reserve | PM1 | 0.007644 | -78.643765 | 2566 | 188 |
| El Pahuma Orchid Reserve | PM2 | 0.007646 | -78.638745 | 2620 | 189 |
| El Pahuma Orchid Reserve | PM3 | 0.005814 | -78.634716 | 2701 | 215.25 |
| Yanacocha Biological Reserve | YNC1 | -0.118017 | -78.590288 | 3500 | 433 |
| Yanacocha Biological Reserve | YNC3 | -0.11817 | -78.586165 | 3573 | 99 |
| Yanacocha Biological Reserve | YNC4 | -0.118829 | -78.586388 | 3639 | 117 |
| Yanacocha Biological Reserve | YNC2 | -0.121873 | -78.586031 | 3789 | 448 |
| Yanacocha Biological Reserve | YNC6 | -0.127453 | -78.585937 | 3792 | 70 |
| Yanacocha Biological Reserve | YNC7 | -0.133951 | -78.586264 | 3827 | 70 |

Table S4. Locations of 47 point-count survey sites.

| Location | Site | Elevation | Latitude | Longitude |
|------------------------------|-------------|------------------|-----------------|------------------|
| Mindo Road | MD1350 | 1350 | -0.046417 | -78.774912 |
| Mindo Road | MD1400 | 1400 | -0.043631 | -78.774174 |
| Mindo Road | MD1450 | 1450 | -0.039735 | -78.768298 |
| Mindo Road | MD1500 | 1500 | -0.036381 | -78.763184 |
| Tandayapa Valley | TV1550 | 1550 | -0.032102 | -78.76027 |
| Tandayapa Valley | TV1600 | 1600 | -0.032194 | -78.756172 |
| Tandayapa Valley | TV1650 | 1650 | 0.008767 | -78.675107 |
| Tandayapa Valley | TV1700 | 1700 | 0.001142 | -78.677465 |
| Tandayapa Valley | TV1750 | 1750 | -0.002424 | -78.676523 |
| Tandayapa Valley | TV1800 | 1800 | -0.004994 | -78.67931 |
| Tandayapa Valley | TV1850 | 1850 | -0.007302 | -78.679387 |
| Tandayapa Valley | TV1900 | 1900 | -0.009187 | -78.677998 |
| Tandayapa Valley | TV1950 | 1950 | -0.008935 | -78.674577 |
| Tandayapa Valley | TV2000 | 2000 | -0.01162 | -78.676167 |
| Tandayapa Valley | TV2050 | 2050 | -0.011607 | -78.676781 |
| Tandayapa Valley | TV2100 | 2100 | -0.014528 | -78.678841 |
| Tandayapa Valley | TV2150 | 2150 | -0.015446 | -78.678564 |
| Tandayapa Valley | TV2200 | 2200 | -0.016471 | -78.680287 |
| Tandayapa Valley | TV2250 | 2250 | -0.033772 | -78.711801 |
| Tandayapa Valley | TV2300 | 2300 | -0.020286 | -78.680745 |
| Tandayapa Valley | TV2350 | 2350 | -0.020713 | -78.685011 |
| Puluhua Geobotanical Reserve | PLH2450 | 2450 | 0.03963 | -78.505067 |
| Puluhua Geobotanical Reserve | PLH2500 | 2500 | 0.041178 | -78.50699 |
| Puluhua Geobotanical Reserve | PLH2550 | 2550 | 0.041542 | -78.508211 |
| Puluhua Geobotanical Reserve | PLH2600 | 2600 | 0.038624 | -78.506736 |
| Puluhua Geobotanical Reserve | PLH2650 | 2650 | 0.038916 | -78.508792 |
| Puluhua Geobotanical Reserve | PLH2700 | 2700 | 0.038145 | -78.510321 |
| Puluhua Geobotanical Reserve | PLH2750 | 2750 | 0.035932 | -78.508509 |
| Puluhua Geobotanical Reserve | PLH2800 | 2800 | 0.030719 | -78.507268 |
| Puluhua Geobotanical Reserve | PLH2850 | 2850 | 0.032584 | -78.509352 |
| Puluhua Geobotanical Reserve | PLH2900 | 2900 | 0.029954 | -78.508985 |
| Puluhua Geobotanical Reserve | PLH2950 | 2950 | 0.026022 | -78.509418 |
| Puluhua Geobotanical Reserve | PLH3000 | 3000 | 0.022693 | -78.506682 |
| Puluhua Geobotanical Reserve | PLH3050 | 3050 | 0.02128 | -78.503247 |
| Yanacocha Biological Reserve | YNC3200 | 3200 | -0.136919 | -78.595753 |
| Yanacocha Biological Reserve | YNC3200 | 3250 | -0.135987 | -78.595114 |
| Yanacocha Biological Reserve | YNC3300 | 3300 | -0.135544 | -78.594339 |
| Yanacocha Biological Reserve | YNC3350 | 3350 | -0.13593 | -78.593872 |
| Yanacocha Biological Reserve | YNC3400 | 3400 | -0.135263 | -78.593229 |
| Yanacocha Biological Reserve | YNC3450 | 3450 | -0.135304 | -78.592771 |
| Yanacocha Biological Reserve | YNC3500 | 3500 | -0.116594 | -78.589738 |
| Yanacocha Biological Reserve | YNC3550 | 3550 | -0.11761 | -78.585957 |
| Yanacocha Biological Reserve | YNC3600 | 3600 | -0.118021 | -78.586189 |
| Yanacocha Biological Reserve | YNC3650 | 3650 | -0.118625 | -78.586638 |

| Location | Site | Elevation | Latitude | Longitude |
|------------------------------|-------------|------------------|-----------------|------------------|
| Yanacocha Biological Reserve | YNC3700 | 3700 | -0.119843 | -78.586115 |
| Yanacocha Biological Reserve | YNC3750 | 3750 | -0.121073 | -78.585723 |
| Yanacocha Biological Reserve | YNC3800 | 3800 | -0.12267 | -78.585154 |